CHARLES UNIVERSITY IN PRAGUE

FACULTY OF SCIENCE

DIPLOMA THESIS

Markéta Bocková

Study of biomolecular interactions by the method of surface plasmon resonance

Supervisors: Assoc. Prof. Jiří Homola, Ph.D.,DSc.

RNDr. Tomáš Kučera, Ph.D.

Prague 2009

I would like to thank Prof. Jiří Homola, Ph.D., DSc. and RNDr. Tomáš Kučera, PhD. for valuable advice and kind help during my work.
Furthermore I thank my colleagues from the Institute of Photonics and Electronics for pleasant collaboration.
My greatest thanks is to my family, friends and especially to my husband for support and patience.

I declare that submitted thesis is entirely my own work created under the guidance of Prof. Jiří Homola, Ph.D., DSc. and RNDr. Tomáš Kučera, Ph.D. and all sources used have been referenced accordingly.

Prague, 4. 9. 2009

Markéta Bocková

Contents

List of abbreviations

17β – HSD10	17β-hydroxysteroid dehydrogenase type 10
a-HSD 10	antibody against 17β-hydroxysteroid dehydrogenase type 10
Aβ	amyloid β peptide
$Aβ_{40}$	amyloid β (sequence of 1–40 amino acids)
$Aβ_{17-24}$	amyloid β (sequence of 17-24 amino acids)
ABAD	amyloid β peptide alcohol dehydrogenase
ACSF	artificial cerebrospinal fluid
AD	Alzheimer disease
ATR	attenuated total reflection
BSA	bovine serum albumin
BdO_{23}	biotin-$(triethylenglycol)_2$-5'-d(CAG TGT GGA AAA TCT CTA GCA GT)-3'
CSF	cerebrospinal fluid
EA	ethanolamin hydrochlorid
EDC	1-ethyl-3-(3-dimethylaminopropyl)-carbodiimide hydrochloride
EG	ethylenglycol
ELISA	enzyme-linked immunosorbent assay
ERAB	endoplasmic reticulum-associated binding protein
HADH	L-3-hydroxyacyl-CoA dehydrogenase
Mism4	5'-ACT GCC AGA AAT TCT CCA TAC TG-3'
MS	Multiple sclerosis
NAD^+	nicotinamide adenine dinucleotide
NHS	N-hydroxysuccinimide
NMR	nuclear magnetic resonance
ON	oligonucleotide
PBNa	high ionic strength phosphate buffer
PBS	phosphate buffer
SA	sodium acetate buffer
SAM	self-assembled monolayer
SCHAD	short-chain L-3-hydroxyacyl-CoA dehydrogenase
SP	surface plasmon

SPR	surface plasmon resonance
$Tris_x$	Tris buffer

1 Introduction

The study and characterization of biomolecular interactions became an important part of medicine research and diagnostic, drug discovery and applications of molecular biology and biochemistry. In addition, in many important research areas there is a need for accurate and rapid detection and identification of chemical or biological compounds. Surface plasmon resonance (SPR) based biosensors are rapid and allow the direct detection of biomolecular interactions without the need of labeling.

Among other sensor technologies, e.g. those based on electrochemical [1] or piezoelectric principle of action [2], the optical biosensors are advantageous because of their high sensitivity. Next advantage of optical biosensor measurements is that they do not require any electrical signal in a sensing area and cannot be perturbed by electric or magnetic field [3-5].

SPR biosensors have become a widely used technology for both analysis of various analytes and study and characterization of molecular interactions such as antibody-antigen, DNA-DNA, DNA-protein, protein-protein, receptor-ligand and protein-membrane interactions [6-9]. The ability to real time and direct measurements affords to quantitatively determine kinetic or thermodynamic parameters or to investigate binding stoichiometry or epitopes presented on the antigen [10-13].

Due to capability of SPR biosensors to direct detection of molecules in various media, SPR biosensors can provide a new insight into interactions involved in medical diagnostics on molecular basis, development and therapy [14-17] and are utilized in numerous important fields including environmental monitoring [18-20] and food safety [21-23].

1.1 Surface plasmon resonance method

Surface plasmon resonance (SPR) biosensors belong to the family of refractometric affinity biosensors. The SPR biosensors are based on the measuring of the changes in characteristics of a localized electromagnetic wave – a surface plasmon (SP). In SPR biosensor, the SP is excited at the interface between a thin metal film (most often gold) and

a dielectric medium. SP propagates along the metal-dielectric interface and intensity of SP electromagnetic field decays exponentially from the metal surface to a dielectric medium. The penetration depth of the SP field is 200-400 nm depending on the configuration of SPR biosensor. One of the characteristics of an electromagnetic wave, the propagation constant, is highly influenced by changing of refractive index in the close proximity of the metal surface [24]. A refractive index change can be generated, for instance, by the binding of biomolecules (analyte) to their biospecific partners (receptors) immobilized on the sensor surface. SPR biosensor measures the changes in the propagation constant of the SP and thus it determines the relative amount of bound analyte on the biosensor surface. Based on which particular parameter is the change of propagation constant measured, the SPR biosensors are classified as SPR biosensors with wavelength, angular, intensity, phase, or polarization modulation [25].

The excitation of SP based on the principle of attenuated total reflection (ATR) with the utilization of an optical prism as a coupling element is one of the most frequent strategies of SP excitation. In such SPR biosensors (with wavelength modulation) a beam of polychromatic light is brought to the thin metal film under a constant angle of incidence and excites an SP (Fig. 1, left).

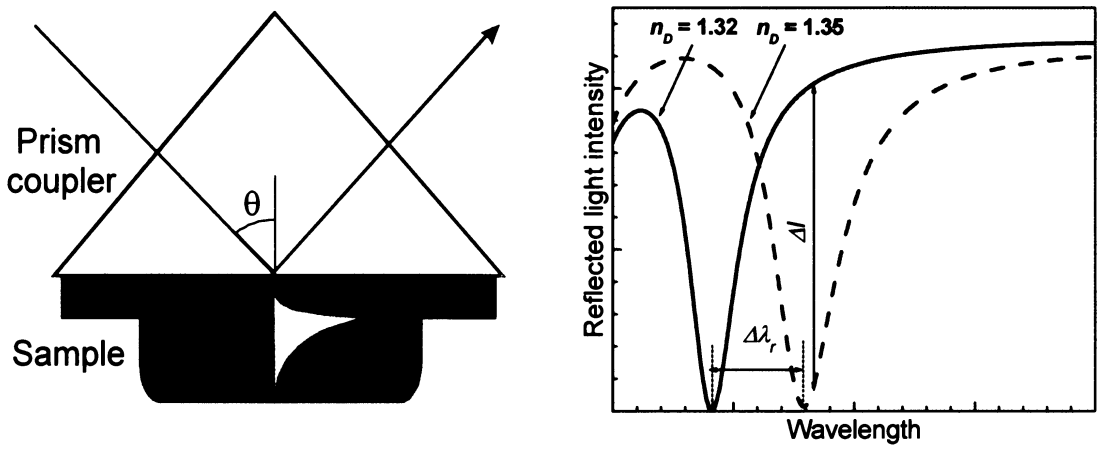

Figure 1: Excitation of the surface plasmons via prism coupler (left). Intensity of reflected light as a function of wavelength for a fixed angle of incidence (curves for two different refractive indices of the sample) (right).

The SP propagation constant is measured by intensity of reflected light in wavelength spectrum and for the wavelength at which the energy of incident light is transferred into SP is observed characteristic dip in spectrum of reflected light. The shift

inresonant wavelength is proportional to the refractive index change at the sensor surface and thus to surface concentration of captured biomolecules (Fig. 1, right, page 6).

Typical SPR biosensor response to the analyte binding to receptor immobilized on the sensor surface is shown in Figure x as a plot of the shift in resonant wavelength versus time. Three phases of the single measurement can be distinguished: (1) buffer flowing along the sensor surface until the stable baseline is achieved (Fig. 2, phase I.), (2) analyte solution is flowed across the sensor surface - interaction with immobilized receptor is observed (Fig. 2, phase II.), (3) washing the sensor surface with the same buffer as before the analyte injection – dissociation of analyte-receptor complex can be monitored (Fig. 2, phase III.). The amount of bound analyte at the sensor surface is determined as the distinction in the sensor response between the equilibrium level after washing the bound surface with buffer (at the end of phase III.) and the baseline level obtained when the same buffer was flowed before the injection of the analyte solution (at the end of phase I.). The SPR biosensor response can be calibrated to provide the surface concentration of bound molecules. The calibration coefficient is proportional to their molar weight [26] and depends on the resonant wavelength.

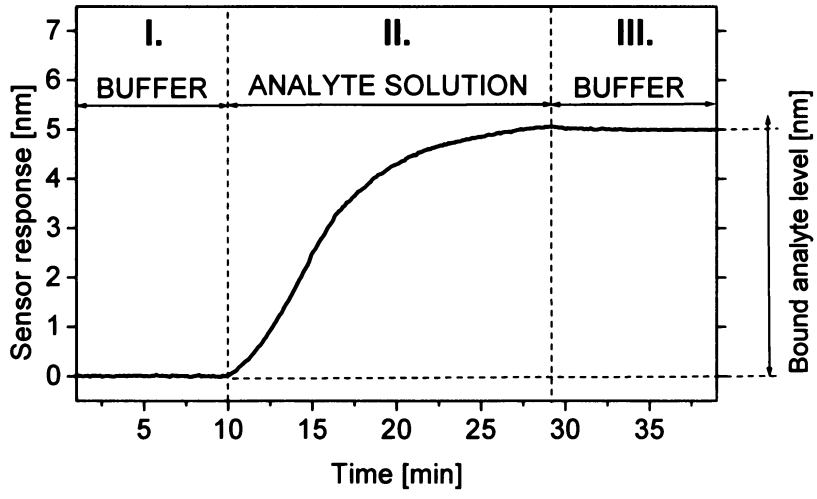

Figure 2: Typical SPR biosensor response to continuous measurement of analyte binding to immobilized receptors. The sensor surface with immobilized receptors is washed with buffer (phase I), then the analyte-receptor complex formation is observed (phase II), finally the same buffer as it was used in the phase I is flowed across the surface (phase III).

1.1.1 Immobilization methods

In SPR biosensor, one of the interacting biomolecule (receptor, biomolecular recognition element) is immobilized on the metal surface and interacts with its biospecific partner (analyte) in solution. Immobilization of receptors on the surface should be considered during the development of biosensor, because the method of receptor attachment significantly affects the resulting sensor sensitivity and specificity of the analyte detection.

Various types of biomolecules such as antibodies or their fragments [27, 28], peptides [29], DNA or RNA aptamers [30, 31] or molecularly imprinted polymers [32] have been used as the receptors. The aim of the immobilization is to achieve a defined and sufficiently high density of immobilized receptors without loss of their biological activity and availability of functional groups for their direct immobilization, and to prevent non-specific binding of analyte and other molecules from solution onto the sensor surface.

Methods of immobilization of receptors on gold films exploit physico-chemical interactions such as chemisorptions [33], covalent binding [34, 35], hydrophobic and electrostatic interactions [36], and high-affinity biomolecular linker systems (e.g. streptavidin–biotin [37, 38], proteins A or G [39], histidine tagged protein - chelated metal ions [40] and complementary oligonucleotides [41]).

In principle, the molecules can be immobilized either on the surface or in a three-dimensional matrix. The latter provides more binding sites than immobilization on the surface, relatively non-fouling background and environment for the preservation of immobilized molecules during prolonged storage. The most widely used three-dimensional matrix is the carboxymethylated dextran [42]. However, the binding of analyte molecules to the immobilized receptors may be slowed down due to the diffusion of analyte through the hydrogel matrix [43]. For surface (two-dimensional) immobilization the self-assembled monolayers (SAMs) have been widely used. To achieve a desired surface density of receptors along with reducing of non-specific binding, SAMs mixed of long-chained (n=12 and higher) n-alkylthiols terminated with functional group for further attachment of receptors and of short-chained alkylthiols terminated with ethylenglycol or hydroxylic groups for a non-fouling background, have been utilized [44].

Immobilization via covalent attachment to carboxylic/ethylenglycol SAMs is suitable for immobilization of proteins and other molecules containing primary amines. Other strategies for protein immobilization were summarized in several publications [45].

There are several strategies for oligonucleotide (ON) immobilization onto gold sensor surface, e.g. assembly of thiol-terminated ONs directly on the surface [46, 47] or binding of biotinylated ONs to the streptavidin via a highly affinitive streptavidin-biotin interaction [48, 49]. Streptavidin is a tetrameric protein (60 kDa) obtained from bacteria Streptomycea Avidinii. Dissociation constant of the complex streptavidin - biotin is in the order of 10^{-15} M, which is one of the strongest known non-covalent interactions. Each streptavidin molecule has four binding "pockets" for biotin [50], Figure 3.

Figure 3: Scheme of streptavidin tetramer with four biotin molecules (yellow) bound in four binding pockets.

Other approaches to immobilization of ONs on gold surfaces are mentioned for instance in [38].

1.1.2 Kinetic aspects of SPR method

Understanding of kinetic parameters of biomolecular interactions is an important point in the characterization of biological systems. Considerable effort has been focused on biomolecular interactions analysis in the research and industrial areas such as the drug development, functional protein analysis and applications where preparation and purification of biomolecules is performed. One of fundamental characteristics of these

interactions relies on the kinetics of association and dissociation processes. SPR biosensors are a unique technology that allows the reaction kinetics monitoring in real time. This is commonly considered one of the greatest advantages of the SPR method.

SPR biosensors measure time behavior of the relative changes in molecular mass in the close proximity of the sensor surface. In a typical reaction in SPR biosensor, the interaction between surface bound receptor (R) and analyte in solution (A) is studied. An interaction between A and R can be described as reaction:

$$A + R \underset{k_d}{\overset{k_a}{\leftrightarrow}} AR \tag{1}$$

where AR is the product of their association and k_a resp. k_d is association resp. dissociation kinetic rate constant, which characterizes given reaction and is time and analyte concentration independent. Equation (1) describes two simultaneous processes: the association, where A and R form a single complex AR, and dissociation, where the AR complex dissociates into two separate parts A and R. For the association the distance between A and R need to be lower than the critical radius. It is assumed that the probability of the complex formation is the same for each molecule. This assumption vanishes the influence of molecular orientation and speed of translation and rotation.

Mathematical model is based on kinetic equation that describes how the amount of formed/dissociated complexes depends on the local concentrations of the free analyte and the free/bound receptors. Assuming that the concentration of the analyte is maintained constant (by either continual replenishment by flowing analyte solution along the sensor surface or by the use of a sufficiently high analyte concentration) the interaction between the A and R may be described by pseudo-first-order kinetics [51], which was originally derived by Langmuir for interactions freely proceeding in solution

$$\frac{d\gamma}{dt} = k_a \alpha_0 (\beta - \gamma) - k_d \gamma \tag{2}$$

where γ is the surface concentration of the complexes formed per unit time, α_0 is the concentration of the analyte and β is the surface concentration of the receptors. Thus $\beta - \gamma$ is the amount of free unbound receptors. Both β and γ are expressed in the same way in terms of local density. Equation 2 is formally identical with the equation describing a first-order reaction in solution, therefore is referred to as pseudo first-order kinetics.

The kinetics of pseudo-first order is typical for flow cell based SPR sensors. Thus the concentration of the analyte can be stepwise increased at the beginning to a concentration of α0 and then immediately reduced to zero [52]. After the stepwise increase in the concentration of the analyte and after a sufficient time period the association and dissociation come into equilibrium and the equilibrium constant may be determined [53]

$$K = \frac{k_a}{k_d} = \frac{\gamma_{eq}}{\alpha_0(\beta - \gamma_{eq})} \tag{3}$$

In real molecular systems, the processes in the active molecular layer can be more complicated. Sensor response is then the superposition of several parallel or subsequent reactions. To achieve sufficient accuracy of kinetic parameters is then necessary to use the appropriate (and often much more complex) kinetic model.

1.2 Nucleic acids

There are two classes of nucleic acids (NAs): deoxyribonucleic acid (DNA) and ribonucleic acid (RNA). The basic function of DNA is to store the genetic information essential for reproduction and development of organisms and RNA has various biological functions, e.g. is important in the production of proteins.

The genetic information, encoded in base sequence of DNA, is transferred in the process of DNA replication, transcription into messenger RNA (mRNA) and translation, the mRNA-directed biosynthesis of polypeptides (Fig. 4).

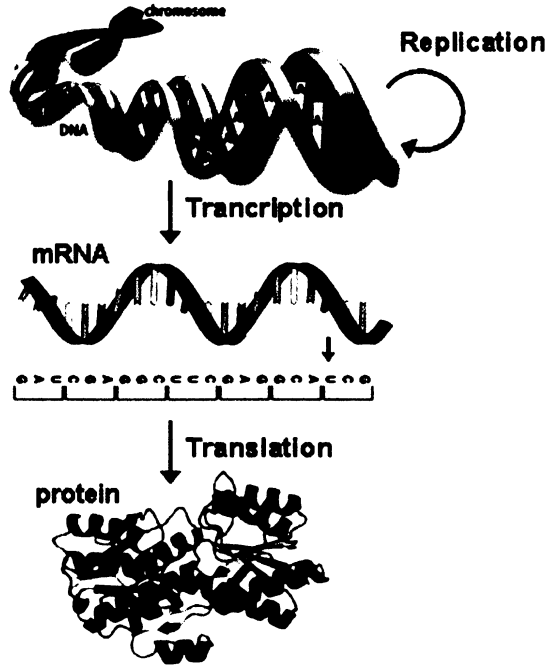

Figure 4: Transfer of genetic information (adapted from [54]).

The structure of NA is formed by a sugar-phosphate backbone and nitrogen-containing bases that are attached to the sugar moiety via an N-glycosidic bond. In RNA, the sugar moiety is ribose and 2'-deoxyribose in DNA. The DNA structure is composed of four types of bases: guanine (G), cytosine (C), adenine (A) and thymine (T). In RNA structure, the thymine is replaced with uracil (U). The specific base pairing is a key to storage and transfer of genetic information. In 1953, James Watson and Francis Crick revealed [55] that in DNA double-helix (duplex) adenine binds only thymine by two hydrogen bonds while guanine forms a pair only with cytosine (by three hydrogen bonds),

Figure 5. Non-Watson-Crick base pairing with different inter-base interactions can occur, e.g. in triple-stranded helices. Such a pairing scheme is Hoogsteen base pairing [56], which occur almost entirely between homopurine and homopyrimidine strands and may have parallel or antiparallel structure [57]. It is expected that the triple helices have a regulatory function in gene transcription. In addition to stable Watson-Cricks base pairs (A·T and G·C), there are other eight possible pairs of these 4 bases, which form complexes of different structure and stability: A·A, A·C, C·C, C·T, G·G, G·A, G·T and T·T, called non-complementary pairs or mismatches. In the DNA pairing, mismatches may occur by replication error, by heteroduplex forming, by spontaneous deamination or by mutagenic chemicals and ionizing radiation [58]. Mismatches are also found in secondary structures of single stranded DNA viruses [59].

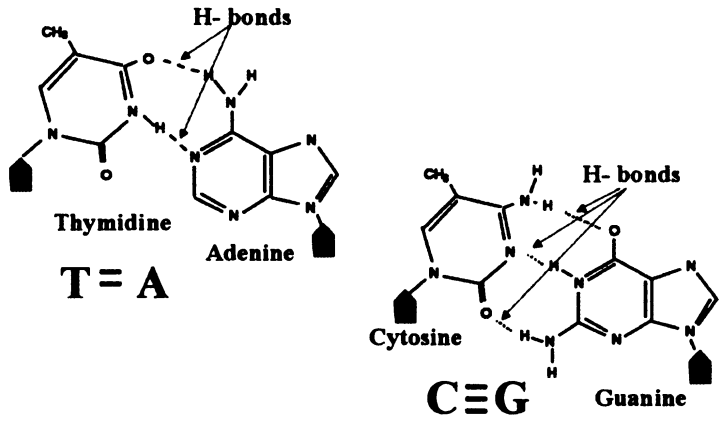

Figure 5: Watson-Crick base pairing (adapted from [60]).

Hydrogen bonds play a substantial role in the functionality of NA, but they are not the main stabilizing factor of three-dimensional structure of DNA. The DNA structure is stabilized by base stacking (interactions of π – electrons of aromatic cycles of bases located above each other in double-helix) and by ionic and hydrophobic interactions.

Geometry of NA in solution is not rigid, but is affected by many factors, such as base composition, NA concentration, fiber length, temperature, ionic strength, etc. [61, 62]. In general, we distinguish several basic forms of NA duplexes: most commonly known is the right-handed B-form of DNA – DNA duplexes under physiological conditions, right-handed A-form is preferred by of DNA – DNA duplexes under dehydrating conditions or

by RNA – RNA duplexes under physiological conditions and left-handed Z-form DNA – DNA duplexes at high salt concentrations (Fig. 6).

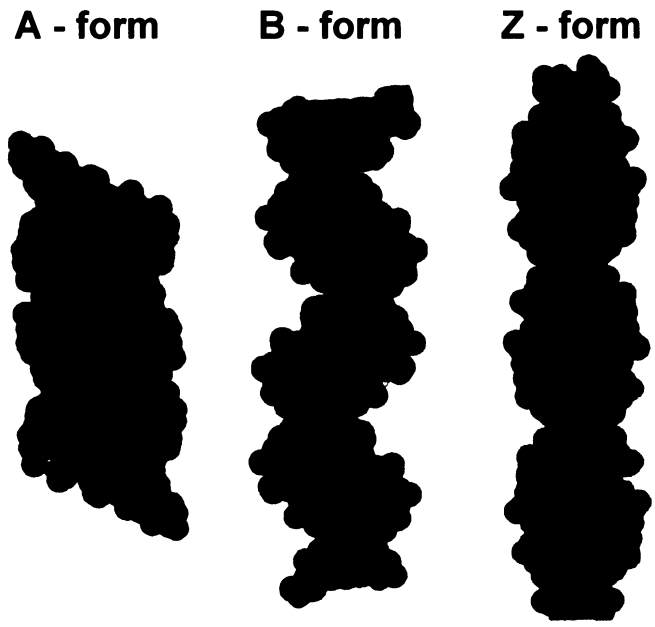

Figure 6: Basic forms of NA duplexes (from left to right): A-RNA, B-DNA and Z-RNA (adapted from [63]).

Due to its chemical, physical and biological activities, NAs are employed in many biosensors and bioanalytical methods. Hybridization reaction is today routinely exploited in a wide range of molecular biology techniques such as polymerase chain reaction, DNA sequencing, blotting techniques or DNA microarrays [64, 65]. These methods depend on highly sensitive and specific detection of hybridization between short synthetic oligonucleotides (ON) and the target nucleic acid sequences in the sample.

Moreover, a large number of research groups have focused on development of strategies for gene therapy that rely on oligonucleotide hybridization such as antisense or antigen therapy [66, 67]. The principle of such therapies is to block the synthesis of proteins, that are essential for the growth of tumor cells or for the reproduction of virus, already at the level of nucleic acids. Due to the instability of DNA oligonucleotides in biological samples, these therapies require the use of their synthetic analogs [9, 68].

NAs and their hybridization are a great source of information that is very important to basic research. Optical biosensors can provide the information on kinetic constants of hybridization reaction [69], on the mechanism of formation of NA complexes [70] or

on conditions affecting their stability [71]. Hybridization thermodynamics and kinetics have been investigated for ONs in solution [72], for gel-bound or nanoparticles-bound ONs [73] and for surface bound ONs [74].

The factors that control NA hybridization have been studied for both perfectly matched and mismatched ONs [75, 76]. Various studies indicate, that hybridization process depends beside ON target sequence also on ON length, temperature, ionic strength or probe density [77-79]. Peterson at al. experimentally confirmed, that hybridization depends strongly on probe density in both the efficiency of duplex formation and the kinetics of target capture [47, 80]. They demonstrated that at higher probe densities the amount of hybridized target decreases and the binding kinetics are slower. Since then several studies focused on immobilizing of ONs at optimal surface density revealed, e.g. [81, 82].

1.3 Alzheimer disease

One of important tools critical to diseases diagnosis, treatment, monitoring and prognosis are biomarkers. Biomarkers can be defined as parameters which mirror the state of organism and serve as indicators for health and disease. The utility of biomarkers consist in their ability to provide an early indication and monitor progression of the disease, and to provide a factor measurable across populations [83, 84]. Fast, sensitive and specific detection of molecular biomarkers indicating normal or pathogenic processes presents an important goal for modern bioanalytics [85, 86].

Alzheimer disease (AD) is an irreversible, progressive and incurable disorder in which brain cells gradually deteriorate, resulting in the loss of cognitive functions. AD is a leading cause of dementia in elderly patients and therefore presents substantial challenge for social and medical care systems of modern societies. Search for efficient diagnostic and therapeutic tools is ongoing worldwide. A wide variety of different proteins such as inflammatory markers, markers of oxidative stress, apolipoproteins, and markers of neuronal degeneration in blood and cerebrospinal fluid (CSF) have been examined in studying AD [87]. The ideal biomarker for AD should be useful in differentiating this type of dementia from other diseases as well as in monitoring the course of the illness. However, a biomarker meeting these criteria has not yet been discovered. Besides imaging methods (a head CT scan, x-ray, positive electron tomography or magnetic resonance imaging) and cognitive tests, the classical clinical diagnostic of "probable" AD uses biochemical analysis of cerebrospinal fluid (CSF) that closely reflects the changes in the composition of the brain. Thus, biomarkers in the CSF should represent the pathogenic processes of AD in the brain. CSF biomarkers of AD include various forms of tau protein and amyloid beta peptide. In the clinical routine, CSF amyloid beta 1–42, total-tau and phosphorylated tau is measured by sandwich ELISAs to discriminate between patients with AD or healthy individuals [88]. Even though the clinical diagnosis has a relatively high accuracy rate (80-90%) [89], reliable diagnosis of AD can only be made post-mortem [90] or by determination of extracellular aggregation of insoluble amyloid beta (plaques) (see Fig. 7, page 16) and intracellular deposits composed of hyperphosphorylated tau protein (tangles) [91, 92]. Therefore, methods based on antemortem detection/quantification of molecular biomarkers present an interesting direction in the development of diagnostic technologies for AD.

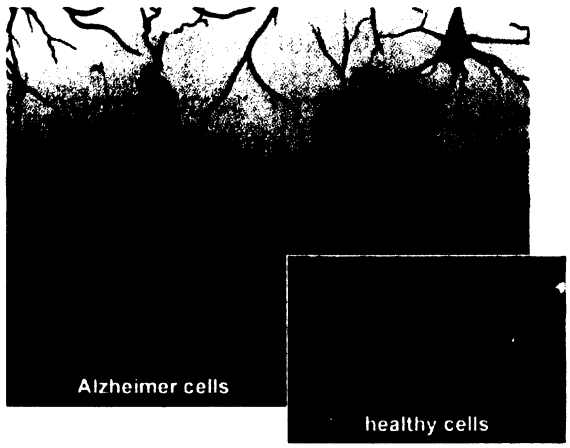

Figure 7: In Alzheimer's disease, the fragments accumulate to form hard, insoluble plaques. In a healthy brain, these protein fragments would be broken down and eliminated (adapted from [93]).

Numerous dysfunctional mechanisms have been described in AD, ranging from protein aggregation and oxidative stress to biometal dyshomeostasis and mitochondrial failure [94, 95]. Recently, attention has focused on the role of mitochondrial dysfunction in AD pathogenesis. Several lines of evidence indicate that intraneuronal accumulation of amyloid beta peptides (Aβs) causes among others mitochondrial dysfunction and neuronal cell death [96]. The mechanisms are not yet fully clear, however, an important role is attributed to the increased opening of mitochondrial pores resulting in release of some mitochondrial enzymes associated with adenosine triphosphate (ATP) production. These ATP production associated enzymes in turn interact with Aβs, which leads to enzyme activities inhibition and their overexpression as a response to maintain the ATP levels and, finally, to apoptotic or necrotic cell death [97, 98].

Intensive research is directed especially towards the mitochondrial 17β-hydroxysteroid dehydrogenase type 10 (17β-HSD10). Reasons are as follows: Aβs specifically and with high affinity interacts with 17β-HSD10 (the dissociation constants are about 40-70 nM) and causes reduced activity of the enzyme in experiments in vitro [99]. Using SPR and saturation transfer difference-NMR experiments, Yan at al. [100] showed that Aβ binding induces conformational and subsequently functional changes in 17β-HSD10 caused by loss of NAD^+. Because NAD^+ is the required cofactor for 17β-HSD10 enzyme activity, Aβs binding results in a loss of 17β-HSD10 function and abolishes the cytoprotective role of17β-HSD10 [101]. The overexpression of 17β-HSD10 was found

especially in cortical and hippocampal regions but not in the cerebellum of patients with AD when compared to age-matched controls [102, 103].

17β-hydroxysteroid dehydrogenase type 10 (17β-HSD10) is multifunctional mitochondrial enzyme that belongs to the short-chain dehydrogenase reductase family of enzymes [104]. First study related to 17β-HSD10 was published by Yan at al. in 1997 [105]. 17β-HSD10 is a homotetramer with a molecular mass of 108 kDa and subunit consisting of 261 amino acid residues (see Fig. 8). In normal tissue the 17β-HSD10 is localized in mitochondria through a N-terminal non-cleavable targeting sequence [106, 107] and concerning to distribution in human tissues, high levels of 17β-HSD10 were observed in heart, brain, kidney and gonads [108].

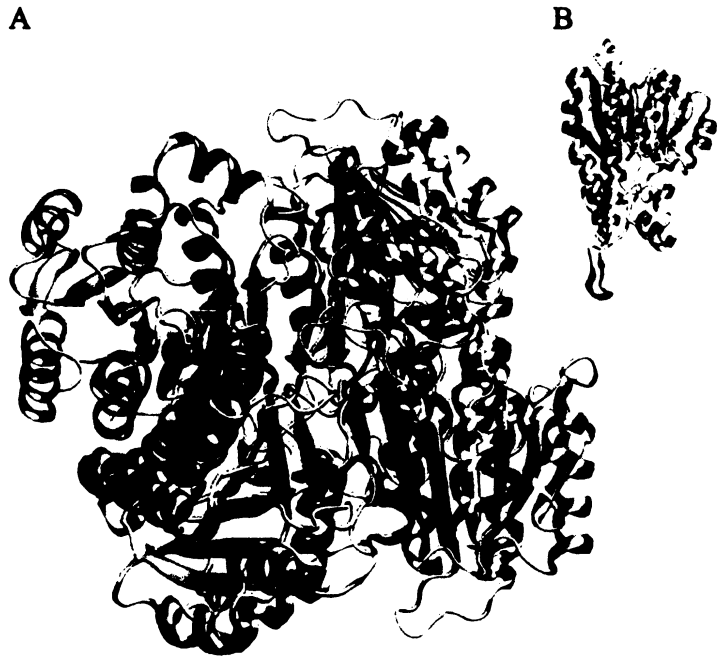

Figure 8: 17β-hydroxysteroid dehydrogenase type 10 tetramer (A) and one of its monomers (B) (adapted from [109]).

17β-HSD10 catalyzes the NAD^+ dependent oxidation and/or reduction at C17 keto/β-hydroxyl groups of a broad set of substrates, e.g. androgen and estrogen hormones [110, 111]. In addition to its catalytic function in steroid hormones metabolism, 17β-HSD10 is also involved in catabolic pathways of straight and branched chain short hydroxyacyl CoA [112]. According to its different activities, 17β-HSD10 is referred to as amyloid beta peptide alcohol dehydrogenase (ABAD), L-3-hydroxyacyl-CoA

dehydrogenase (HADH), short-chain L-3-hydroxyacyl-CoA dehydrogenase (SCHAD) or less appropriately endoplasmic reticulum-associated binding protein (ERAB).

2 Goals

The main goal of this diploma thesis was to master the complex surface plasmon resonance (SPR) biosensor technology and to exploit it for study of selected molecular interactions. Two different classes of molecular interactions were selected for this study – (i) interactions between oligonucleotides and (ii) interaction between proteins, enzymes and peptides involved in the pathogenesis of Alzheimer disease (AD). The study of interactions between oligonucleotides was focused on using the SPR method for determining kinetic parameters of the hybridization process. The main goal of the study of interactions of molecules involved in AD pathogenesis was to design and develop a method allowing for rapid and sensitive detection of the molecules implicated in AD for early diagnostics of AD.

3 Experimental

The experimental work has been carried out at the Institute of Photonics and Electronics of the Academy of Sciences of the Czech Republic. In this chapter, the used surface plasmon resonance (SPR) biosensor technology is described. Reported SPR biosensor was exploited for kinetic analysis of interactions between oligonucleotides. This study was focused on effect of surface probe density on hybridization process. Subsequently, the interactions of molecules involved in pathogenesis of Alzheimer disease were inquired into. The assay for their rapid detection in both buffer and cerebrospinal fluid samples was developed and optimized. Achieved results are presented in sections 4.1 and 4.2.

3.1 Reagents and material

Chemical reagents:

The **$HSC_{11}(EG)_6OCH_2COOH$** (16-mercapto-hexa(ethyleneglycol)hexadecanoid acid) and **$HSC_{11}(EG)_4OH$** (11-mercapto-tetra(ethyleneglycol)undecanol) alkanethiols were purchased from Prochimia, Poland. **$HSC_{11}NH_2$** (11-Amino-1-undecanethiol hydrochloride) alkanethiol was purchased from Probior, Germany. **Streptavidin** from *Streptomycea Avidinii*, bovine serum albumin (**BSA**), **acetic acid,** sodium hydroxide (**NaOH**), **Tween®20** and **triethylamine** were purchased from Sigma-Aldrich, Czech Republic. Ethanolamin hydrochloride (**EA**), 1-ethyl-3-(3-dimethylaminopropyl)-carbodiimide hydrochloride (**EDC**) and N-hydroxysuccinimide (**NHS**) all included in Amine Coupling Kit from Biacore, Sweden. **Absolute ethanol** was purchased from MERC, Czech Republic. **SuperBlock** blocking buffer was purchased from Thermo Scientific, USA.

Buffers:

SA (10mM sodium acetate, pH 5.0), **PBS** (10mM phosphate, 2.9mM KCl, 137mM NaCl, pH 7.4), **PBNa** (10mM phosphate, 2.9mM KCl, 0,75M NaCl, pH 7.4), **$Tris_x$** (10 mM Tris-HCl, pH 7.4, "x" means various amount of added NaCl: 0-1000 mM NaCl), Artificial cerebrospinal fluid (**ACSF**, 150mM NaCl, 3,0 mM KCl, 1,4mM $CaCl_2.2H_2O$, 0,8 mM $MgCl_2.6H_2O$, 1 mM phosphate, pH 7.4). All buffer components were purchased from Sigma-Aldrich, Czech Republic.

Biotinylated deoxyribooligonucleotide probes (23-mers):

BdO_{23}: biotin-$(TEG)_2$-5'-d(CAG TGT GGA AAA TCT CTA GCA GT)-3', where "TEG" is tri(ethylenglycol) and

Mism4: 5'-d(ACT GCC AGA AAT TCT CCA TAC TG)-3'

were purchased from LMFR of Masaryk University in Brno. Both were HPLC purified.

Antibodies and other material:

The anti-human endoplasmatic reticulum amyloid-beta binding protein IgG (**antibody against 17β-HSD10 peptide**) and human beta-amyloid 1-40 (full length) peptide ($A\beta_{40}$) were obtained from Alpha Diagnostic Int., USA. Monoclonal mouse anti-amyloid β 17-24 ($A\beta_{17\text{-}24}$) was purchased from BioSource International, USA. Mouse polyclonal antibody against full-length 17β-HSD10 (**a-HSD10**) was purchase from Abnova, Taiwan. **17β-HSD10 enzyme** was prepared and provided by Dr. Jan Říčný from Prague Psychiatric center Bohnice, Czech Republic and polyclonal rabbit antiserum against chloramphenicol (**As171**) was obtained from Applied Molecular Receptors Group, CIBER of Bioengenieering, Biomaterials and Nanomedicine, IIQAB-CSIC, Barcelona Spain.

CSF samples were obtained from patients undergoing lumbar puncture as a part of their routine diagnostic workup. All subjects or proxy gave written informed consents to participate in the study. All samples of CSF obtained by lumbar puncture were frozen within five hours and stored at -80° C until assayed. Repeated freeze/thaw cycles were avoided.

3.2 SPR instrument

In this work, an biosensor based on the spectroscopy of surface plasmons developed at the Institute of Photonics and Electronics, Prague [24], was used. In this sensor, surface plasmons are excited in the Kretschmann configuration of the attenuated total reflection (ATR) method [113]. In this geometry, broadband light from a halogen lamp is collimated and reflected from a base of the prism to which an SPR chip is attached. The chip contains a thick gold layer on which the excitation of surface plasmons occurs upon the incidence of light from the prism. The light reflected from four areas (sensing channels) on the gold layer is collected via GRIN lenses into four optical fibers and coupled to a four-channel spectrograph. Acquired spectra are analyzed in real time by special software package that

allows determination of the resonant wavelength in each sensing channel [114]. The gold SPR chips made of BK-7 glass were coated with an adhesion-promoting titanium film (1nm thickness) and a gold film (50nm) by electron beam evaporating. Schematic representation of used SPR biosensor is shown in Figure 9.

Within the four-channel SPR instrument, it was possible to control the temperature at which the molecular interactions were monitored. The temperature was stabilized by a Peltier's thermoelectric element installed into a thermally stabilized body and a precision temperature controller (ILX Lightwave, USA). Liquid samples in thin-walled Peek tubing were flowed across the thermally stabilized body. The optical prism and the sensor chip were also in contact with the stabilized body. The accuracy of the temperature setting was 0.2°C (limited by the accuracy of the thermistor calibration). All experiments were performed at a temperature of 25°C.

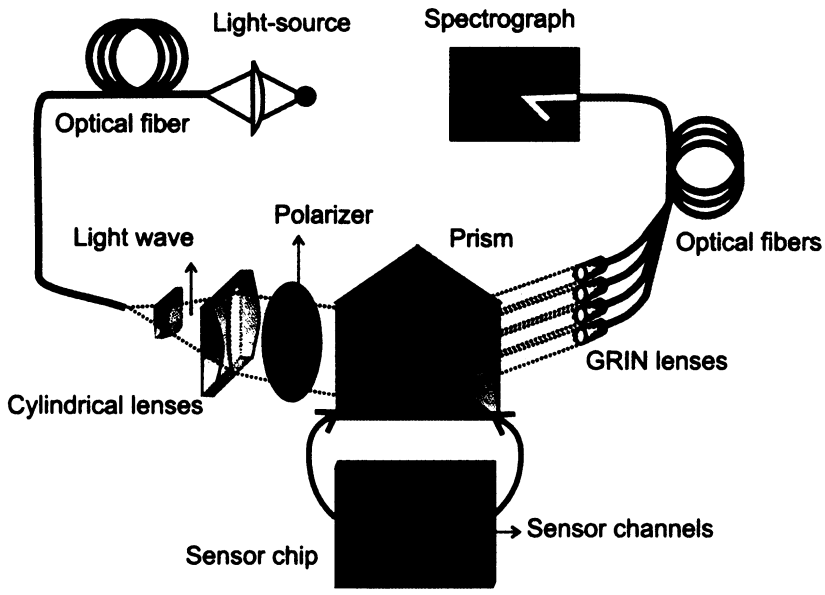

Figure 9: Schematic representation of four-channel SPR biosensor.

The sensor response can be calibrated to provide the surface concentration of bound molecules. The calibration coefficient is proportional to their molar weight [26] and depends on the resonant wavelength. It was estimated from theoretical model that for example a shift in the resonant wavelength of 1 nm corresponds to a change in the surface concentration of streptavidin of about 1.8×10^{11} molecules/cm^2 when measured at the wavelength of 750 nm. It has been shown, that the sensor response per unit mass coverage is comparable for most proteins and single-stranded or double-stranded oligonucleotides [115]. To allow the quantification of all sensorgrams to be comparable,

the sensor responses were recalibrated to the sensitivity at a uniform operating wavelength of 750 nm.

A picture of a four-channel SPR biosensor developed at the Institute of Photonics and Electronics is in Figure 10.

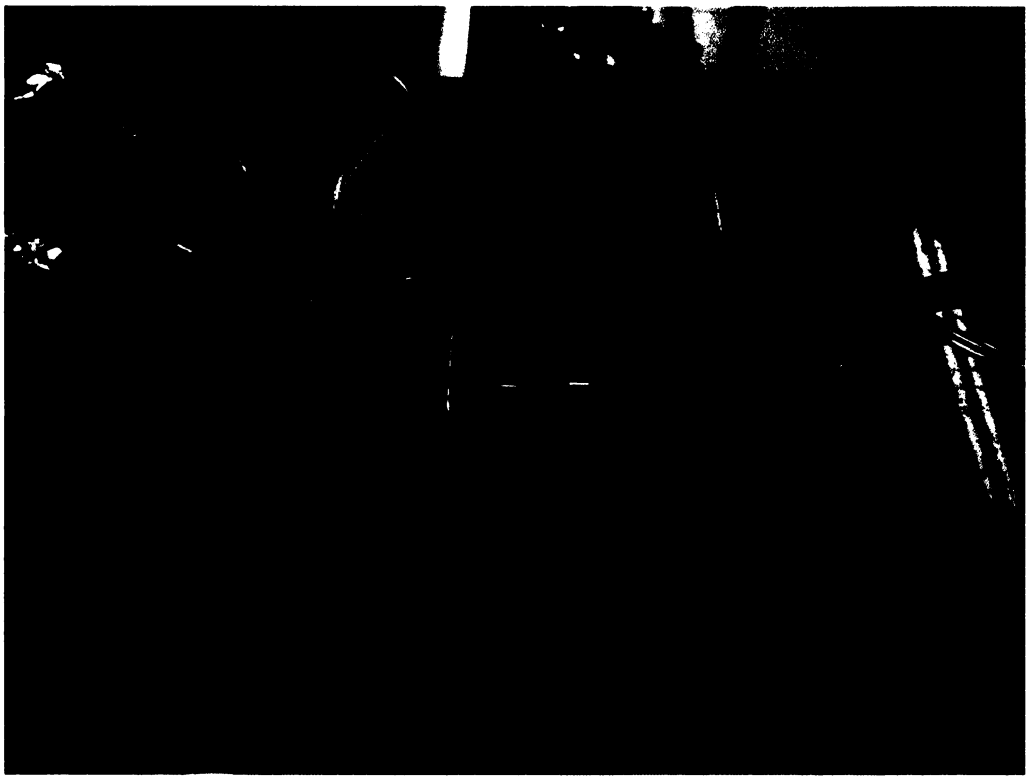

Figure 10: A picture of a four-channel SPR biosensor developed at the Institute of Photonics and Electronics.

3.2.1 Sample delivery system

The used sample delivery system consists of peristaltic pump, flow cell and adjacent options such as microvalves. Within this work, two different fluidic approaches were employed, standard and dispersionless fluidic. In both delivery systems, the liquid sample was continuously flowed through a special flow cell with four separate flow chambers interfaced with the chip to confine the sample during experiments [52]. Each flow chamber was aligned to cover one sensing channel and the volume of each flow cell chamber was

about 1 µl. In order to provide a constant flow of sample over each sensing channel with a desired flow rate, a peristaltic pump was connected to the flow cell. In the reported experiments, the flow rate of 30 µl/min was used.

The schematic representation and picture of standard microfluidic is illustrated in Figure 11. In this approach, the liquid sample is brought to the sensing area through a microfluidic channel and one input and one output port.

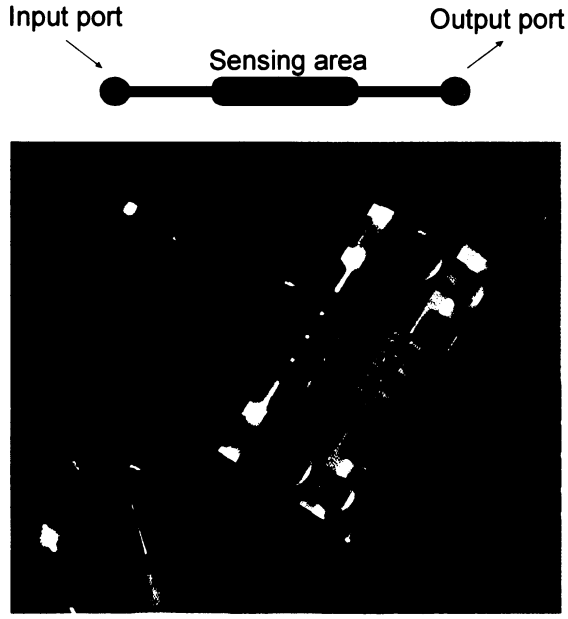

Figure 11: Schematic representation (up) and picture (bottom) of standard microfluidic.

For kinetic study experiments, the dispersionless microfluidic with special microvalves was used to suppress the sample dispersion [116] and intersample mixing [117] (induced by surface effects and high surface-to-volume ratio). The principle of operation of this microfluidic is illustrated in Figure 12, page 25. The sensing area is comprised of a microfluidic channel and two input and two output ports. Two different liquids are introduced to the microfluidic channel through the two input ports. When output port 2 is opened (and output port 1 is closed), liquid #1 flows through the sensing area and then flows to the waste container while liquid #2 flows directly to the waste container (state A). When output port 1 is opened (and output port 2 is closed), the direction of flow is reversed, and only liquid #2 flows through the sensing area (state B). As the injection of the liquid takes place in close proximity to the sensing surface, only very limited liquid dispersion and intermixing occurs before the liquid reaches the sensing area.

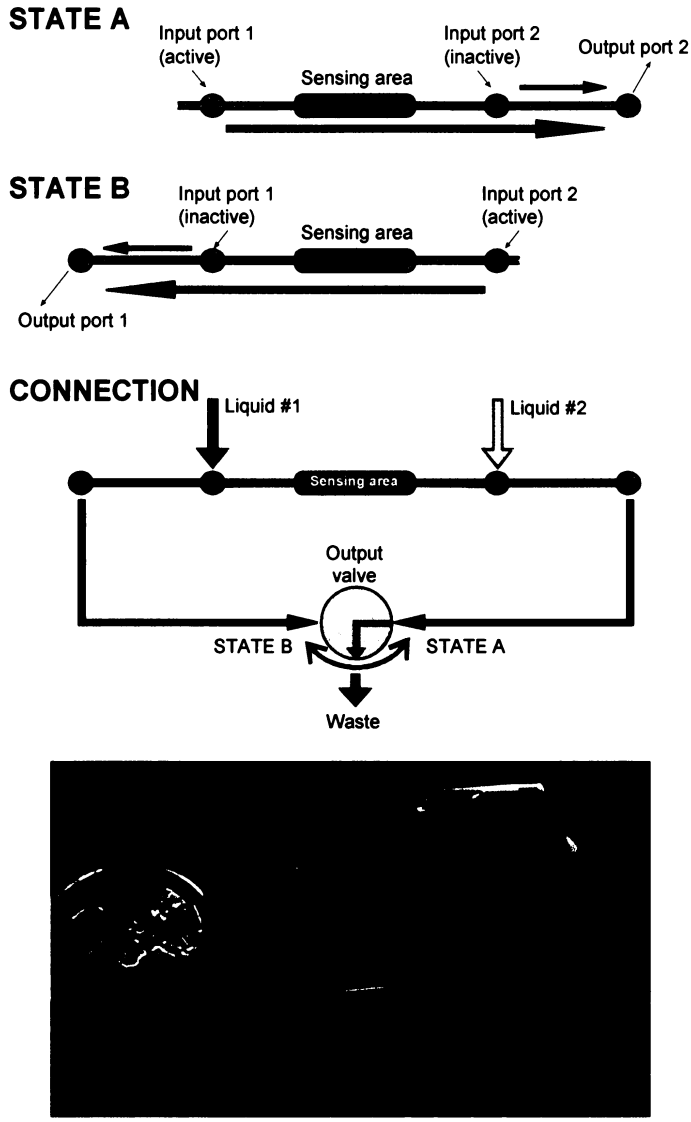

Figure 12: Principle of operation (up) and picture (bottom) of the dispersionless microfluidic.

3.2.2 Functionalization of the sensor chip

The gold SPR chip was cleaned by washing with absolute ethanol, drying with nitrogen stream and by cleaning in UV ozone cleaner for 10 min to remove organic contaminants. The chip surface was washed with deionized water followed with absolute ethanol and dried with a stream of pure nitrogen.

COOH/EG method: The sensor chip was functionalized with a mixed self-assembled monolayer (SAM) by incubating the cleaned gold chip in degassed absolute ethanol with a mixture (7:3) of $HSC_{11}(EG)_4OH$ and $HSC_{11}(EG)_6OCH_2COOH$ alkanethiols with a final concentration of 200 μM. The $HSC_{11}(EG)_6OCH_2COOH$ alkanethiols terminated with

a carboxylic head group were used to anchor a receptor by amino coupling, while $HSC_{11}(EG)_4OH$ alkanethiols terminated with hydroxyl group were used to form a stable non-fouling background. For that purpose the sensor chip was immersed in a mixed thiol solution at a temperature of 40°C for 10 minutes and then stored in a dark place at a room temperature for at least 1 day. After the formation of the mixed SAM, the chip was removed from the solution, rinsed with absolute ethanol and deionized water, and dried with nitrogen. The chip was then immediately mounted to the prism on the SPR sensor. The activation of carboxylic terminal groups was performed *in situ* by injecting deionized water followed by a (1:1) mixture of NHS and EDC (both included in Amine Coupling Kit from Biacore) for 5 minutes and deionized water again. Schematic description of the process is shown in Figure 13.

NH_2 method: The sensor chip was functionalized with a SAM by incubating the cleaned gold chip in degassed absolute ethanol with a $HSC_{11}NH_2$ alkanethiols with a final concentration of 200 μM. The triethylamine was added to final concentration of 3%. Sensor chip was stored in this solution in a dark place at a room temperature for at least 1 day. After the formation of the SAM, the chip was removed from the solution, rinsed with ethanolic solution of acetic acid (10% v/v), absolute ethanol, deionized water and absolute ethanol again and dried with nitrogen. The chip was then immediately mounted to the SPR sensor.

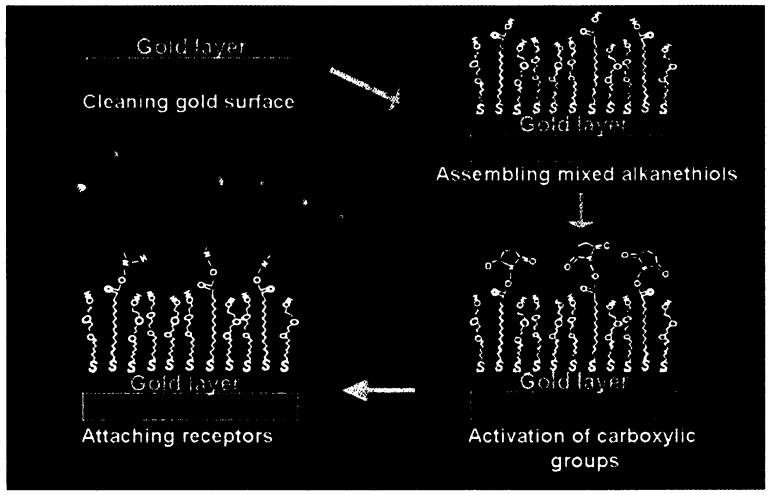

Figure 13: Immobilization of receptors to the sensor surface via COOH/EG method: Clean gold surface was first covered with mixture of alkanethiols to form SAM. After activating the carboxylic group, receptors were attached to the SAM by amide bond formation.

3.2.3 Immobilization of receptors

All immobilizations were performed at a flow rate of 30 µl/min and a temperature of 25°C.

Immobilization via covalent attachment to COOH/EG SAM (amide coupling chemistry) was performed by flowing SA buffer until the baseline was achieved and SA solution with receptor was flowed across the activated surface. Then the SA buffer was injected again. The high ionic strength PBNa buffer was flowed along the sensor surface to remove non-covalently bound receptors and finally, the sensor surface was treated with 1M EA to deactivate residual carboxylic groups.

For immobilization via physical adsorption to positively charged surface of NH_2 SAM, PBS buffer was flowed along the sensor surface until the baseline was achieved then the surface was incubated in PBS solution with receptor for 15 min and PBS buffer was injected again. The sensor surface was treated firstly with PBS + 0.05% Tween®20 to remove all weakly bound receptors and secondly with the SuperBlock blocking buffer to prevent nonspecific binding.

3.2.3.1 Immobilization of oligonucleotides

Immobilization of ONs employed herein was based on covalent attachment of streptavidin to a mixed SAM via amide coupling chemistry followed with biotinylated ON coupling [34]. Schematic illustration of ONs attachment is shown in Figure 14, page 28.

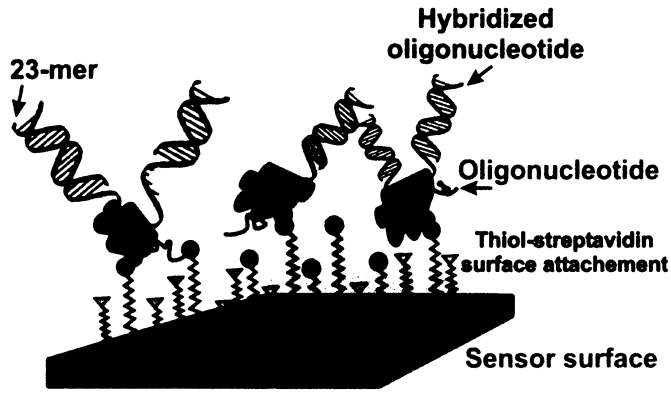

Figure 14: Attachment of oligonucleotides to the SPR sensor surface.

Attachment of streptavidin was performed by means of immobilization of receptors mentioned above in section 3.2.3. Concentration of streptavidin was 50 μg/ml.

For biotinylated ON coupling, $Tris_x$ buffer containing various concentrations of NaCl (0, 50, 150, 300, 500, 1000 mM) was used as immobilization buffer and was flowed along the sensor surface until a baseline was achieved. A 100nM solution of BdO_{23} was then flowed for 15 minutes, or until the saturation was observed, followed with $Tris_x$ buffer injection. Typical sensorgram corresponding to ONs immobilization is shown in Figure 15.

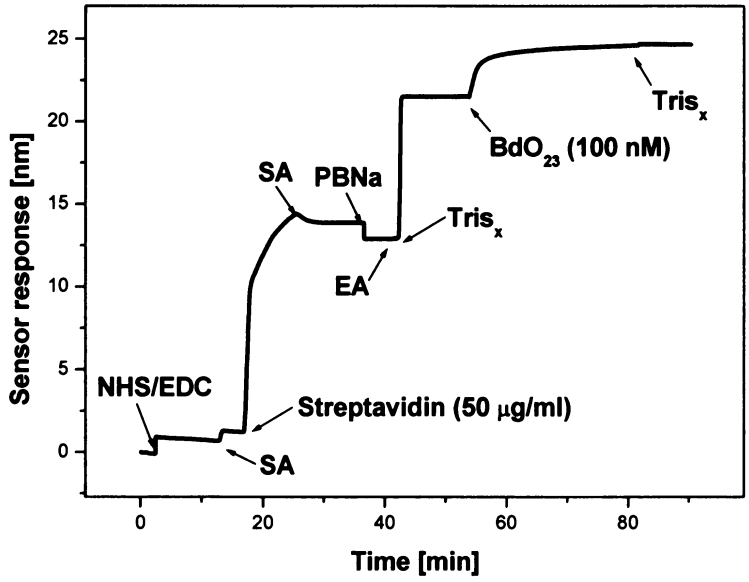

Figure 15: Typical sensorgram corresponding to ONs immobilization.

3.2.3.2 Immobilization of receptors for detection of the molecules implicated in AD pathogenesis

Immobilization methods employed herein were based on attachment of receptors to a SAM via amide coupling chemistry or physical adsorption, respectively, by means of immobilizations described in section 3.2.3.

For direct detection of 17β-HSD10 enzyme, the antibody against 17β-HSD10 peptide or $A\beta_{40}$ was used as receptor. Both were immobilized via covalent attachment to COOH/EG SAM. The antibody at concentration of 20 μg/ml was flowed across the activated surface for 40 minutes, solution with $A\beta_{40}$ (20 μg/ml) for 20 minutes. In order to compensate for non-specific sensor response and thus provide more accurate results, in each binding experiment, one sensing spot was coated with bovine serum albumin (250 μg/ml) as a reference.

The sandwich assay used for determination of 17β-HSD10/Aβs complex levels in CSF was based on binding of the complex to the antibody against $A\beta_{17\text{-}24}$ immobilized on the sensor surface. Both immobilization approaches described in section 3.2.3 were utilized. After $A\beta_{17\text{-}24}$ (4 μg/ml) immobilization, the SuperBlock solution was used to prevent nonspecific binding. In order to compensate for non-specific binding, in each binding experiment, one sensing spot was coated with antibody As171 against chloramphenicol (4 μg/ml) as a reference.

3.3 Analysis of DNA hybridization

For the study of the interactions between oligonucleotides, one oligonucleotide was immobilized on the sensor surface while the other nucleotide contained in a solution was brought in the contact with the SPR sensor.

The immobilized surface was washed with $Tris_{150}$ containing 150 mM NaCl. After a stable baseline was established, the solution with 100 nM partial complementary ON (Mism4) was flowed until the saturation was observed, and then replaced with the $Tris_{150}$ buffer again.

After each hybridization step, the surface was regenerated with injection of $Tris_0$ buffer, which contained no NaCl salt and thus destabilized the formed duplex. The partial complementary ON strand was removed. Then the whole hybridization was repeated.

3.3.1 Kinetic data analysis

Kinetic parameters of hybridization process were determined using BIAevaluation software from Biacore. The analyzed hybridization reaction is 1:1 interaction with high association and dissociation rates. The 1:1 Langmuir pseudo-first-order kinetic model with mass transport was therefore employed (see Fig. 16).

The accuracy of obtained kinetic constants can be determined from so called T-value, which is an estimation of the sensitivity of the fit to changes in the associated parameter. The T-value can be interpreted as a signal-to-noise ratio, meaning that a T-value of 100 corresponds to approximately 1% uncertainty.

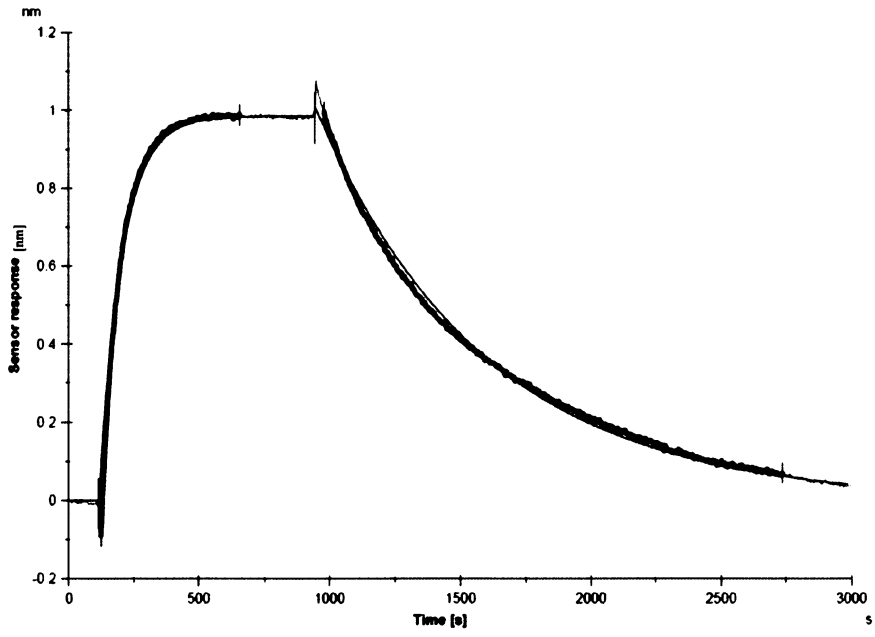

Figure 16: Typical sensor response to hybridization of complementary strand (gray line) and fit with 1:1 Langmuir model with mass transport (black line). Thick areas of the gray curve denote selected data points used for the fitting.

3.4 Detection of the molecules involved in AD pathogenesis

Direct detection of 17β-HSD10 enzyme binding to immobilized antibody or to $A\beta_{40}$ in PBS buffer was performed. Since ACSF more closely mirrors the composition of endogenous CSF than PBS, detection in ACSF was investigated. To determine 17β-HSD10/Aβs complex levels in CSF a sandwich assay was used.

3.4.1 Detection of 17β-HSD10 enzyme

Assay for 17β-HSD10 enzyme was based on 17β-HSD10 enzyme binding to polyclonal antibody against 17β-HSD10 peptide immobilized on the sensor surface (Fig. 17).

Initially, a baseline in PBS buffer was established. Samples of 17β-HSD10 enzyme at increasing concentrations in the range of 1-1000 ng/ml were flowed along sensor surface with captured antibody against 17β-HSD10 peptide and BSA as a reference for 15 minutes. Subsequently, the surface was washed with PBS for 10 minutes.

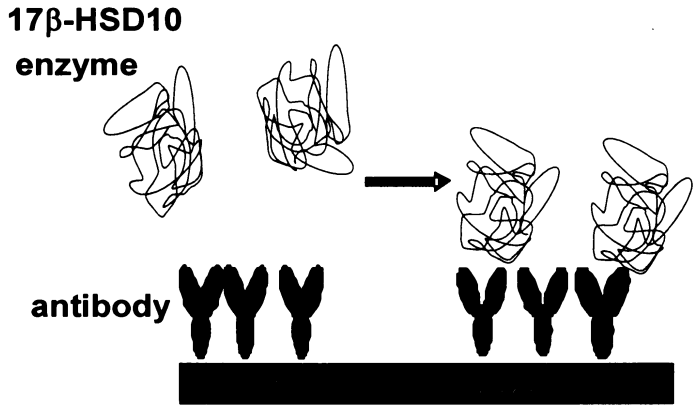

Figure 17: Illustration of assay for detection of 17β-HSD10 enzyme on the immobilized antibody.

In consequent detection experiments, samples containing increasing concentrations of 17β-HSD10 enzyme were sequentially flowed along the surface immobilized with $A\beta_{40}$ (Fig. 18, page 32).

Each solution containing the enzyme was flowed simultaneously along the measuring $A\beta_{40}$ and reference BSA surfaces for 15 minutes. After a short wash-off step

when the PBS was flowed through the flow cell, regeneration reagent (50mM NaOH) was injected for 10 minutes to remove the captured enzyme. Subsequently, PBS was flowed through the flow cell until a stable baseline was achieved. Then, the injection of higher concentration of enzyme was injected.

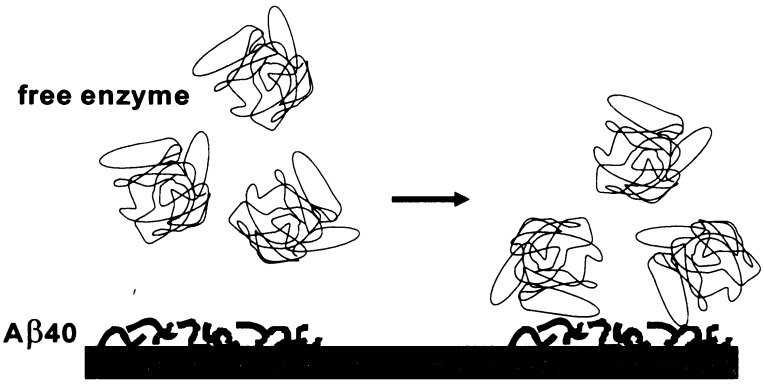

Figure 18: Illustration of assay for detection of 17β-HSD10 enzyme on the $A\beta_{40}$ immobilized surface.

3.4.2 Detection of the 17β-HSD10/Aβs complex

We used a sandwich assay to determine 17β-HSD10/Aβs complex levels in CSF. This assay was based on binding of the complex to the monoclonal antibody against $A\beta_{17-24}$ immobilized on the sensor surface as described above (Fig. 19, page 33).

Initially, a baseline in ACSF was established. Samples of 50% CSF (3x controls, 4x MS, 3x AD) were flowed along the sensor surface with captured antibody against $A\beta_{17-24}$ or As171 as a reference for 20 min and then ACSF was added again. After a short wash-off step when the ACSF was flowed through the flow cell, the second primary antibody to 17β-HSD10 (a-HSD 10) at a concentration of 4 μg/ml was injected for 15 min. Finally, the surface was washed with ACSF.

In order to determine reproducibility of the detection of 17β-HSD10 bound to Aβs in AD sample, sensor response in 4 sensing channels functionalized with antibody against $A\beta_{17-24}$ was analyzed.

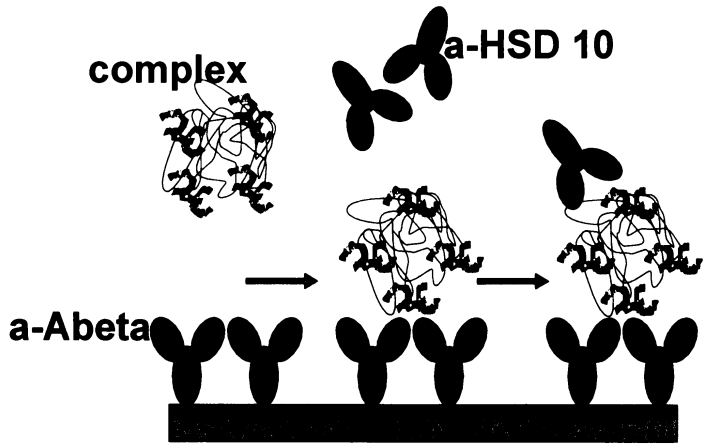

Figure 19: Illustration of assay for detection of 17β-HSD10/Aβ complex.

4 Results and discussion

The surface plasmon resonance method was exploited for study of selected molecular interactions. In this chapter, two areas of results are presented and discussed. Section 4.1 describes analysis of hybridization process of partially complementary short oligonucleotides (ONs) and investigation of the effect of surface probe density on hybridization process. Study of interactions between proteins, enzymes and peptides involved in pathogenesis of Alzheimer disease and detection of these molecules is described in section 4.2.

4.1 Analysis of DNA hybridization

ONs used in this study were short synthetic 23-mers: biotinylated probe BdO_{23} and partially complementary probe Mism4 (for sequences see Experimental part). Duplex of Mism4 and BdO_{23} contains 4 mismatched base pairs, which decrease the stability of the complex and therefore at room temperature of 25 °C considerable dissociation of duplex could be observed.

Following my previous work regarding ONs hybridization [9], optimized version of immobilization chemistry utilizing streptavidin-biotin interaction was employed for ONs probes attachment to obtain high receptor density and hybridization efficiency.

In order to determine SPR biosensor reproducibility of BdO_{23} probes immobilization for on-chip measurements, the sensor response in 3 individual sensing channels on one chip was analyzed. The reproducibility for chip-to-chip measurements was determined from 6 individual sensing channels on 3 different chips (see Fig. 20, page 35). The sensor response to BdO_{23} binding to streptavidin layer showed the reproducibility better than 95% for measurements performed on a single chip and better then 90% for chip-to-chip measurements.

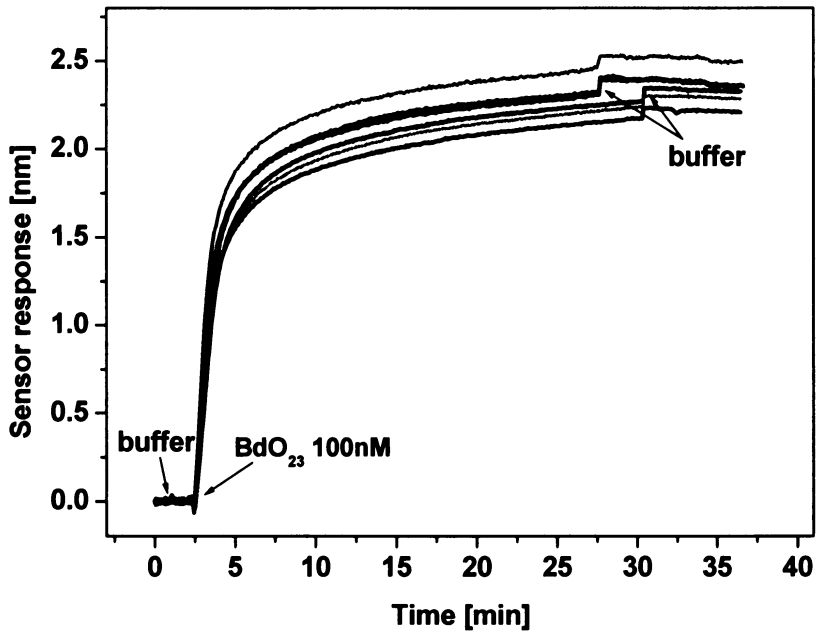

Figure 20: Sensor response to BdO_{23} probe binding to streptavidin layer obtained from six individual sensing channels.

SPR biosensors can provide the information on kinetic constants of hybridization reaction [69] or on conditions affecting their stability [71]. As it was found by Peterson at al. [47], method of the ONs probe immobilization significantly influences the efficiency and kinetics of duplex formation. They also found, that surface probe density is a crucial factor for ONs hybridization efficiency and kinetics. It could be explained by the presence of steric crowding at high probe density [80] or other effects such as electrostatic repulsion of negatively charged phosphates of immobilized probes [82]. The supposed mechanism is such that with immobilization of biotinylated ONs onto the sensor surface the overall negative charge of immobilized ONs gradually increases along with the repulsion of immobilized ONs. At small ions concentrations in immobilizing buffer, where the negative charge of phosphate groups is insufficiently compensated, the repulsion increases over time so that biotinylated ONs can not get close enough to the streptavidin and bind with it. Therefore, surface probe density can be adjusted by ionic strength of immobilization buffer.

To obtain desired surface probe density, $Tris_x$ buffer containing various concentrations of NaCl (0, 50, 150, 300, 500, 1000 mM) was used as immobilization buffer. Dependence of sensor response to binding of BdO_{23} probe on NaCl salt concentration in immobilization buffer is shown in Figure 21.

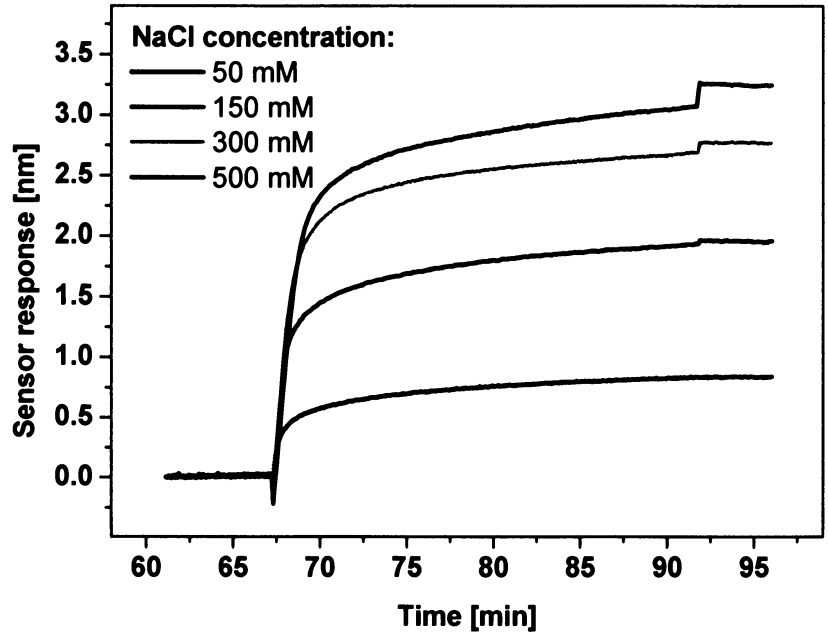

Figure 21: Sensor response to binding of BdO_{23} probe depending on NaCl salt concentration in immobilization buffer.

As follows from this figure, the amount of immobilized probes is highly dependent on the salt concentration. At low ion concentration, very low surface concentration of probes is achived compared to the surface density in buffer with high ionic strength. That is in agreement with assumption, that strong electromagnetic repulsion between polyanionic chains limits the surface density of probes. When NaCl salt is added to the buffer, the natrium cations tend to accumulate in the proximity of anionic deoxyribophosphate chains and therefore decrease the electrostatic repulsion between probes in close proximity. These results are consistent with observations made by Herne and Tarlov [118] who reported that maximum probe coverage is achieved the KH_2PO_4 concentration is above 0.4 M.

The sensor response was calibrated to provide the probe density of bound BdO_{23} probes according to procedure described in experimental section 3.3. Individual probe

densities corresponding to NaCl salt concentrations in immobilization buffer are listed in Table 1.

Table 1: BdO_{23} probe densities corresponding to NaCl salt concentrations in immobilization buffer

NaCl salt concentration (mM)	**BdO_{23} probe density** (10^{12} molecules/cm^2)
50	1.2
150	2.6
300	4.3
500	4.8
1000	5.3

It was demonstrated, that reported BdO_{23} immobilization procedure is reliable and high reproducible method how to achieve an optimum surface probe density without the need of e.g. varying the time for immobilization or controlling immobilization via electrostatic field as described in [47].

After preparation of surface with various BdO_{23} probe densities, the hybridization process and influence of surface probe density on this process was investigated. For all hybridization study experiments, the dispersionless microfluidic was used to suppress the sample dispersion and intersample mixing.

For monitoring of hybridization of Mism4, $Tris_{150}$ hybridization buffer was used. The regeneration procedure described in experimental section 3.3.2 enabled to remove target molecules (Mism4) from immobilized probes (BdO_{23}) without loss of its sensitivity to the next ONs hybridization detection for at least 6 cycles (data not shown here). Thus ON duplex formation could be observed several times on one single chip.

Sensor response to hybridization of Mism4 to probes immobilized in various surface probe densities is shown in Figure 22, page 38. This figure as well represents modeled curves obtained from BIAevaluation software. It is clear, that due to different densities of immobilized probes different saturation levels of hybridized Mism4 were achieved. It was also observed that dissociation process, which depends only on amount of immobilized probes, differed for individual surface probe densities.

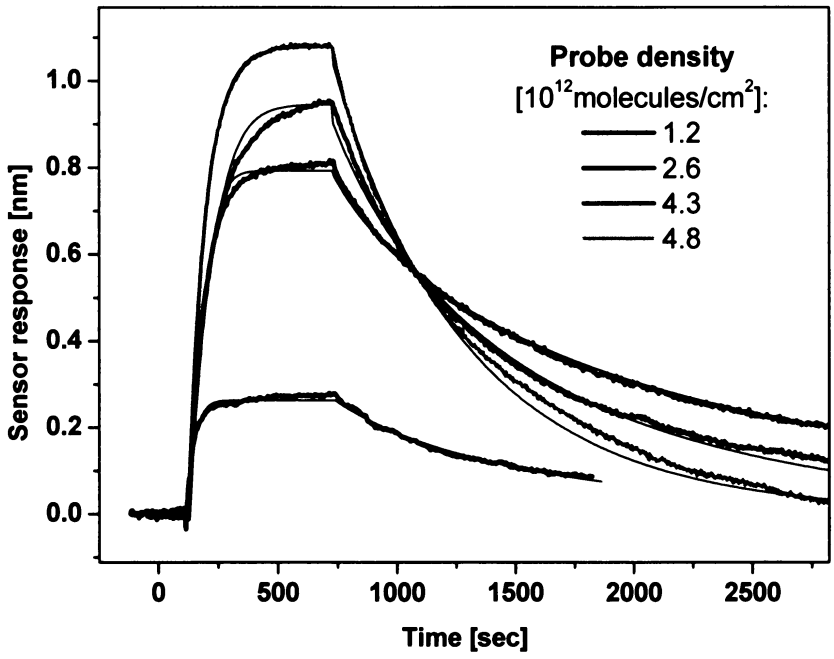

Figure 22: Sensor response to hybridization of Mism4 to BdO_{23} probes immobilized in several surface densities. Modeled curves were obtained from BiaEvaluation software.

4.1.1 Kinetic analysis of hybridization process

An important parameter for quantifying the hybridization reaction and stability of formed duplex is association equilibrium constant. Several research groups were focused on effect of surface probe density on hybridization efficiency (e.g. [69, 80, 115]).

In Figure 23, page 39, there is displayed the dependence of association equilibrium constant of surface-bound Mism4* BdO_{23} duplexes on surface density of BdO_{23}. The values of equilibrium constants were obtained from BIAevaluation software. The trend represented by this data demonstrates, that the stability of formed Mism4* BdO_{23} duplexes decreases with increasing surface probe density in approximately linear dependence. However, to obtain precise relation between duplex stability and surface density of probes, more detailed measurement would be necessary.

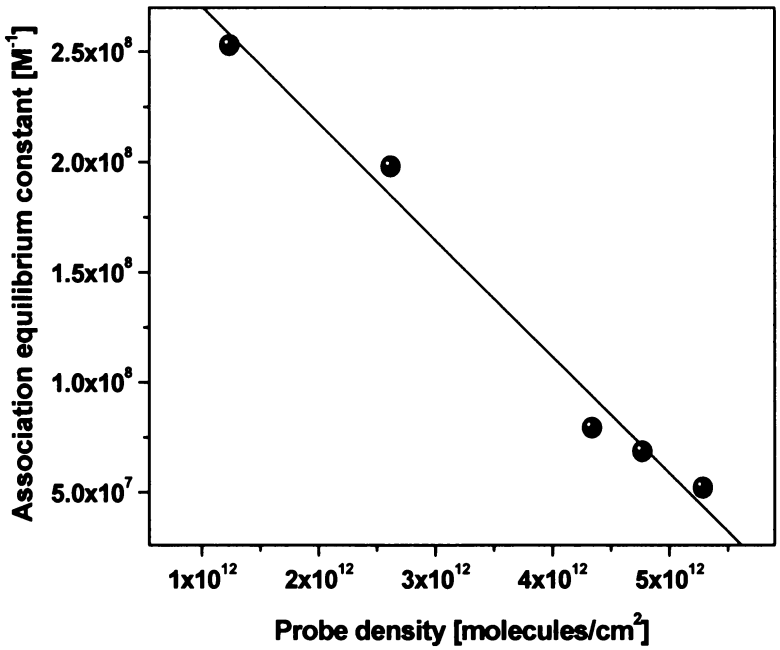

Figure 23: Dependence of association equilibrium constant of surface-bound Mism4* BdO_{23} duplexes on surface density of BdO_{23}.

Dependence of association and dissociation rate constants on surface probe density is presented in Figures 24 and 25, page 40. As follows from these Figures, both association and dissociation contribute to the decreasing trend of association equilibrium constant of duplexes. The decreasing trend of association rate constant confirms results presented by Peterson at al. [47, 80]. They quantitatively established that for probe densities below $3x10^{12}$ molecules/cm^2, the association rate was faster reaching a saturation level within 15 minutes than for high densities above $5x10^{12}$ molecules/cm^2.

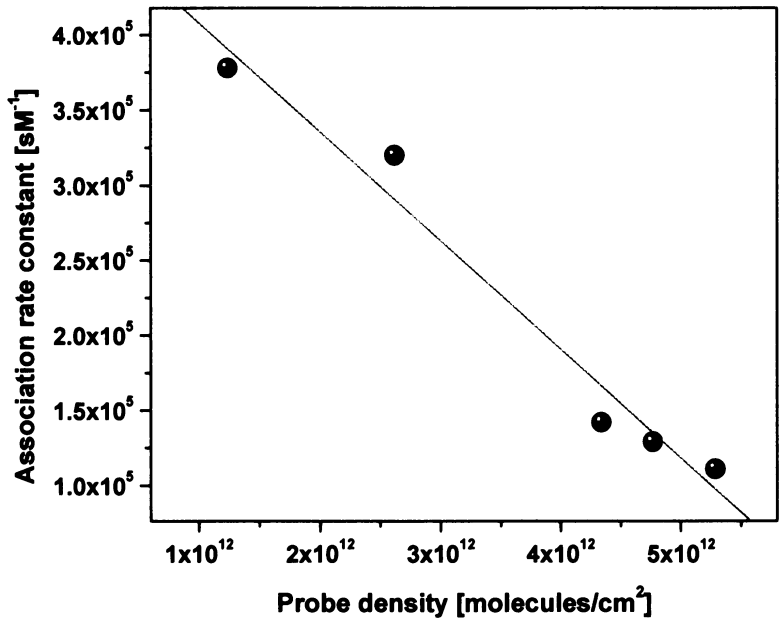

Figure 24: Dependence of association rate constant of surface-bound Mism4* BdO_{23} duplexes on surface density of BdO_{23}.

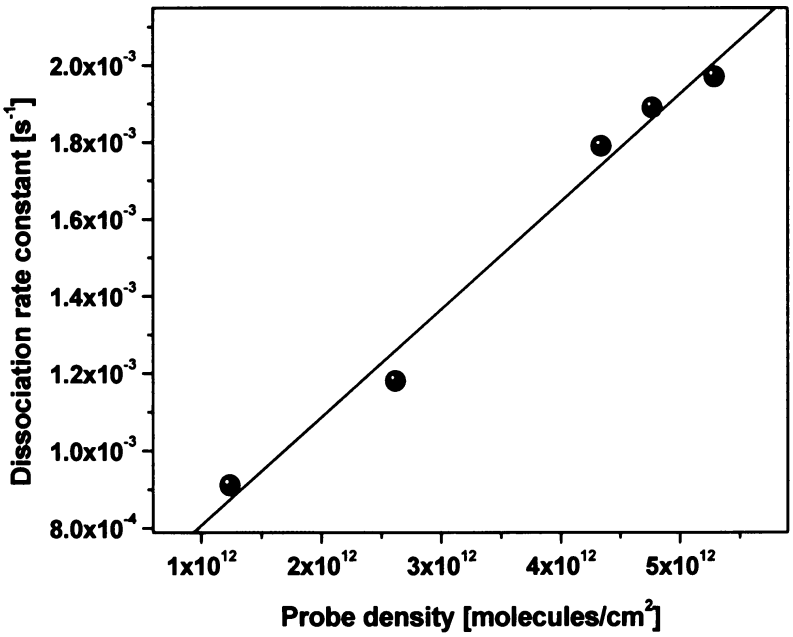

Figure 25: Dependence of dissociation rate constant of surface-bound Mism4* BdO_{23} duplexes on surface density of BdO_{23}.

It was shown, that surface probe density of immobilized probes strongly effect hybridization process and formation of partial complementary short ONs duplexes. To investigate this effect in real time, the SPR biosensor was used. The kinetic analysis of ONs hybridization was performed and association equilibrium constant and association and dissociation rate constants were assumed. Also dependence of constants on surface probe density was determined.

4.2 Study of molecules involved in Alzheimer disease pathologenesis

The investigated interactions of 17β-HSD10 enzyme, amyloid β peptides and 17β-HSD10/Aβs complex are discussed here.

In the first step, the assay for detection of 17β-HSD10 was developed and optimized. Subsequently, the formation of 17β-HSD10/Aβ complex was studied. Specificity of changes in relation to 17β-HSD10/Aβs complex levels in CSF of patients suffering with AD or multiple sclerosis (MS) compared to the controls were evaluated. Various functionalization methods, immobilization approaches and experiment conditions were investigated.

4.2.1 Detection of 17β-HSD10 enzyme

The 17β-HSD10 enzyme at increasing concentrations in the range of 1-1000 ng/ml was flowed along sensor surface with attached antibody against 17β-HSD10 peptide. Typical sensorgram corresponding to the binding of 17β-HSD10 enzyme at different concentrations is shown in Figure 26, page 43. As follows from this figure, the response of the sensor to 17β-HSD10 enzyme binding is rather low and even the concentration of 1000 ng/ml could not saturate binding sites on the sensor surface. Together with relatively high detectable concentration (100 ng/ml of enzyme), these experiments indicate low antibody - enzyme affinity. Thus this assay could not be utilized for sensitive detection of 17β-HSD10 enzyme and another approach had to be tested.

Due to high affinity binding of amyloid β peptides to 17β-HSD10, the $A\beta_{40}$ peptide was chosen as a receptor and immobilized to a COOH/EG SAM via amide coupling chemistry. Detection of 17β-HSD10 enzyme in PBS buffer was then accomplished as follows: 17β-HSD10 enzyme was brought to the $A\beta_{40}$ coated sensor surface and the 17β-HSD10/$A\beta_{40}$ complex formation was observed. Specific sensor response to binding of different concentrations of 17β-HSD10 enzyme is shown in Figure 27, page 43.

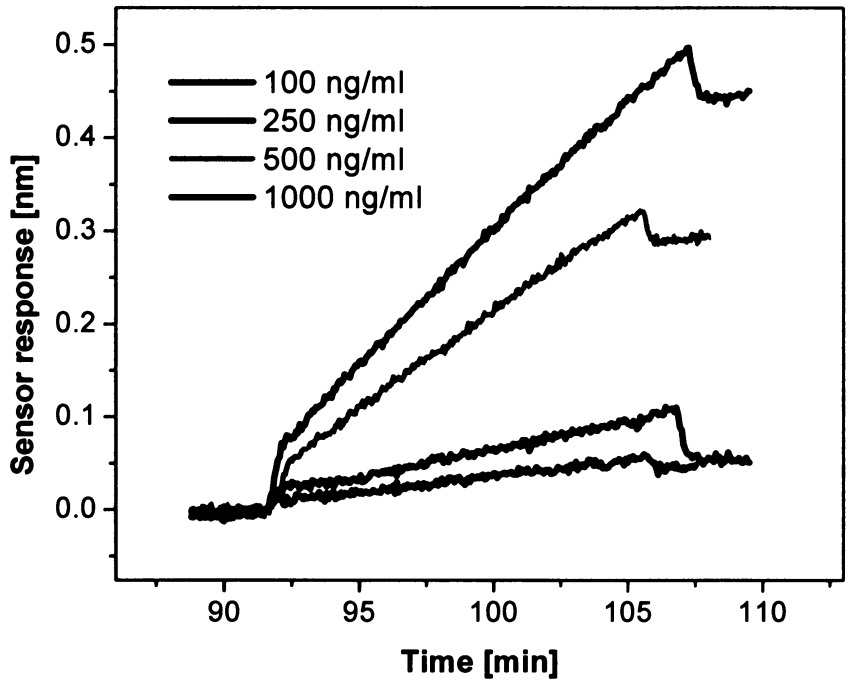

Figure 26: Sensor response to 17β-HSD10 enzyme binding to antibody against 17β-HSD10 peptide immobilized on the sensor surface.

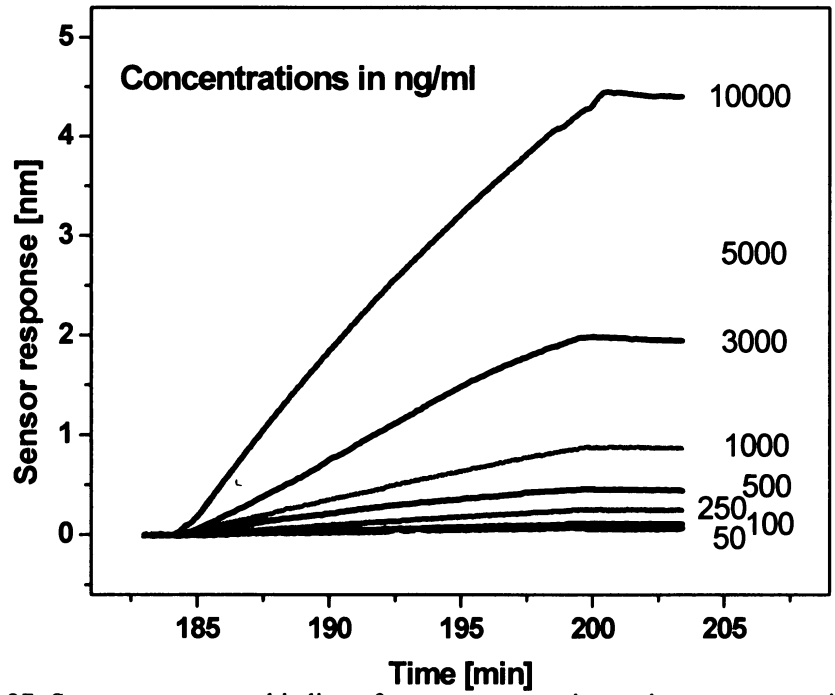

Figure 27: Sensor response to binding of increasing concentrations of 17β-HSD10 enzyme in PBS.

When sensor response to 17β-HSD10 enzyme binding on immobilized antibody and on $A\beta_{40}$ was compared, the levels of $A\beta_{40}$-bound 17β-HSD10 enzyme were almost twice higher then in the case of antibody. However, even this approach did not afford desired sensitivity. Thus, the detection of 17β-HSD10 enzyme on immobilized $A\beta_{40}$ in artificial cerebrospinal fluid (ACSF) was performed. Clearly, the detection in ACSF as a more natural environment provides higher response than the same concentration of enzyme in PBS buffer. Calibration curves of SPR sensor obtained from sensor response to a series of different concentrations of 17β-HSD10 enzyme in PBS and ACSF are shown in Figure 28. The standard deviations ware calculated from the sensor response to the set of measurements on different chips.

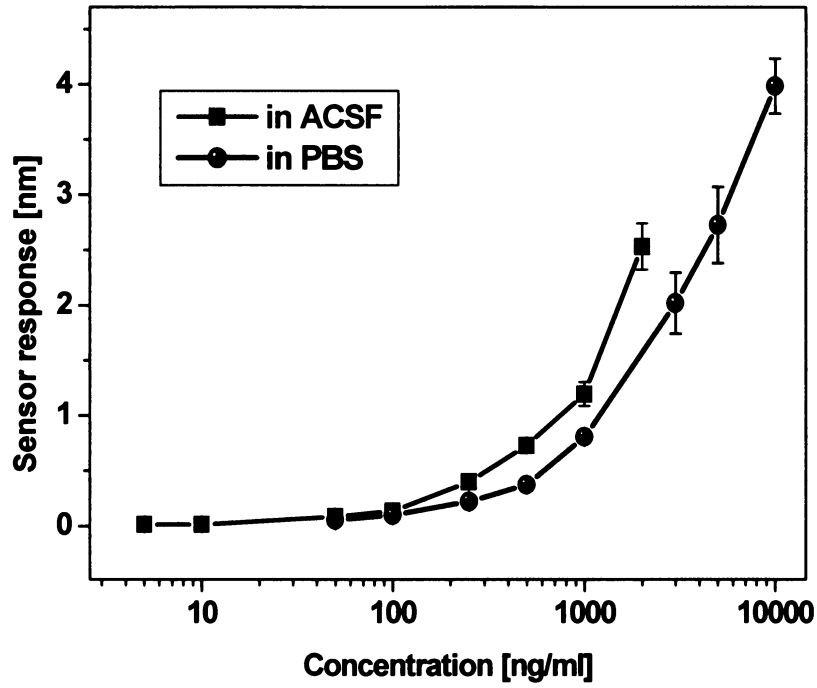

Figure 28: Calibration curves. Sensor response to different concentrations of 17β-HSD10 enzyme in PBS and ACSF binding to $A\beta_{40}$ peptide immobilized on the sensor surface.

Limit of detection was determined as a 17β-HSD10 enzyme concentration for which the sensor response was equal to three standard deviations of the baseline noise. As follows from Figure 28, the limit of detection for 17β-HSD10 enzyme in PBS was estimated to be 50 ng/ml. When performing detection in ACSF, lower concentrations of 17β-HSD10

enzyme could be detected. For detection of 17β-HSD10 enzyme in ACSF the limit of detection was determined at 5 ng/ml.

Assay for rapid and sensitive detection of 17β-HSD10 enzyme was developed and detection experiments in ACSF demonstrated that the reported SPR biosensor is capable of detecting 17β-HSD10 enzyme at ng/ml levels. Results of these experiments were published in [119].

4.2.2 Detection of the 17β-HSD10/Aβs complex

To measure the levels of 17β-HSD10 bound to Aβs, the sandwich assay was used. The antibody recognizing residues 17-24 in the middle region of Aβs ($A\beta_{17-24}$) was immobilized on the sensor chip, i.e. all natural fragments should be taken from CSF (however, the antibody also recognizes the precursor forms and the abnormally processed isoforms). Two different methods for immobilization of antibody against $A\beta_{17-24}$ were tested. Both immobilization via covalent attachment to COOH/EG SAM and immobilization via physical adsorption to positively charged surface of NH_2 SAM. Although the advantage of latter one is simplicity and very high level of immobilized receptors, low resistance to non-specific binding from complex media such as CSF was substantial limitation. Even surface blocking by SuperBlock solution did not screen out positive charge which caused non-specific binding. For this reason, immobilization via amide coupling chemistry providing stable surface with good resistance to non-specific binding, was used. 50% CSF samples (3x controls, 4x MS, 3x AD) were flowed along the surface with captured antibody against $A\beta_{17-24}$ and a-HSD10 antibody was subsequently added.

As it is obvious from Figure 29, page 46, there was the moderately increased sensor response in patients suffering with AD and moderately decreased sensor response in patients with MS when compared to the controls. Levels of 17β-HSD10 bound to Aβs were estimated in CSF of three controls, of four patients with multiple sclerosis (MS) and of three patients with Alzheimer disease (AD). The sensor response to 50% CSF showed reproducibility better than 89% for measurements performed on a single chip.

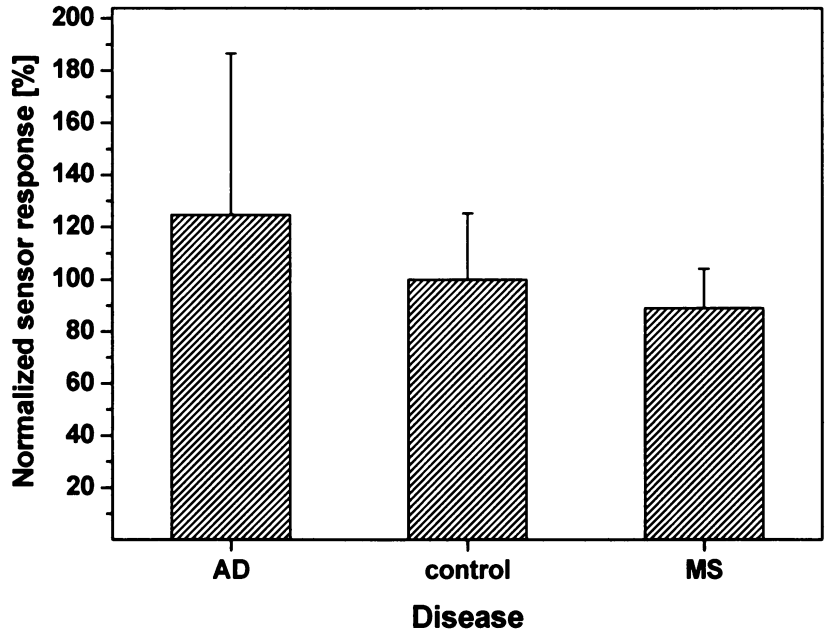

Figure 29: Levels of 17β-HSD10 bound to Aβs in CSF estimated by means of sandwich assay

The levels of 17β-HSD10 enzyme bound to Aβs were significantly increased only in patients with AD thus it is supposed that evaluations of these complexes could be benefitial in AD diagnostic.

It was demonstrated, that with proper immobilization chemistry, the SPR biosensor is capable to detect molecules involved in AD pathogenesis from 50% CSF samples. Results of these experiments were published in [120].

5 Conclusion

Within this diploma work, surface plasmon resonance (SPR) biosensor technology was exploited to study interactions between biomolecules. In particular, the work was focused on the study of hybridization of partially complementary synthetic oligonucleotides and interactions between proteins, enzymes and peptides involved in pathogenesis of Alzheimer disease.

For the study of the interactions between oligonucleotides, one oligonuclotide was immobilized on the surface of the SPR sensor while the other oligonucleotide contained in a solution was brought in the contact with the SPR sensor. The method of immobilization of oligonucleotide probes on the SPR sensor surface was optimized to achieve an optimum surface probe density. It was shown, that surface probe density can be varied by changing the ionic strength of the immobilization buffer and higher probe coverages can be obtained by using high concentrations of ions which screen the electrostatic repulsion between the probes. It was found out, that the surface probe density plays an important role in the study of hybridization process. Different hybridization kinetics were observed at different surface probe densities The kinetic analysis of hybridization process revealed that the association equilibrium constant decreases with the increasing surface probe density. This effect was attributed to the electrostatic repulsion between the hybridizing oligonucleotides.

The study of interactions of the molecules involved in pathogenesis of Alzheimer disease focused on 17β-HSD10 enzyme, amyloid β peptides and 17β-HSD10/Aβs complex. In the first step of the study, methods for the immobilization of amyloid β peptides and antibodies against the 17β-HSD10 enzyme and amyloid β peptides were developed and optimized in terms of binding capacity of the resulting biomolecular coatings. Subsequently, assay for rapid and sensitive detection of 17β-HSD10 enzyme was developed and the limit of detection for 17β-HSD10 enzyme in artificial cerebrospinal fluid (CSF) was determined at 5 ng/ml. It was also demonstrated that the developed method is capable of detecting 17β-HSD10/Aβs complex in CSF samples with reproducibility better than 89%. Finally, CSF samples from patients suffering with AD, multiple sclerosis and healthy controls were compared an it was reveled the patients with AD exhibited elavated levels of 17β-HSD10 enzyme bound to Aβs compared to the two other groups..

This diploma thesis evidences the capacity of SPR biosensor technology for real-time analysis of biomolecular interactions and illustrates the potential the technology holds for other important application areas, such as medical diagnostics. The research reported in this thesis resulted in two publications in peer-reviewed scientific journals and five presentations at international conferences.

6 Relevant publications by Markéta Bocková

- Z. Krištofiková, **M. Bocková**, K.Hegnerová, A. Bartoš, J. Klaschka, J. Říčný, D. Řípová, J. Homola: Enhanced levels of mitochondrial enzyme 17ß-hydroxysteroid dehydrogenase type 10 in patients with Alzheimer disease and multiple sclerosis, Molecular Biosystems, in print, available online, **DOI:** 10.1039/b904799a
- K. Hegnerová, **M. Bocková**, H. Vaisocherová, Z. Krištofiková, J. Říčný, D. Řípová, J. Homola: Surface plasmon resonance biosensors for detection of Alzheimer disease biomarkers, Sensors and Actuators B-Chemical. 139, 69-73 (2009)

- K. Hegnerová, **M. Bocková**, Z. Krištofiková, J. Říčný, D. Řípová, J. Homola: Optické biosenzory s povrchovými plazmony a biomarkery Alzheimerovy nemoci, XIV. Celostátní conference biologické psychiatrie s mezinárodní účastí, Luhačovice 2009
- Z. Krištofiková, K. Hegnerová, **M. Bocková**, A. Bartoš, J. Říčný, D. Řípová and J. Homola: Analysis of the complex between amyloid beta peptides and mitochondrial enzyme 17beta-HSD10 in cerebrospinal fluid, 33rd FEBS congress, Athens 2008
- D. Řípová, Z. Krištofiková, A.Bartoš, J. Říčný, K. Hegnerová, **M. Bocková** and J. Homola: Could be levels of mitochondrial enzyme 17β-HSD10 in cerebrospinal fluid a new biomarker of Alzheimer disease?, Oslo 2008
- K. Hegnerová, **M. Bocková**, H. Vaisocherová, Z. Krištofiková, J. Říčný, D. Řípová, J. Homola: Surface plasmon resonance biosensors for detection of Alzheimer disease biomarkers, Europtrode IX, Dublin, 2008
- Z. Krištofiková, D. Řípová, P. Hovorková, A. Hořínek, E. Majer, J. Homola, H. Vaisocherová, **M. Bocková**, and K. Hegnerová: Amyloid beta – binding protein 17beta-hydroxysteroiddehydrogenase type 10 and Alzheimer disease, III Meeting on the Molecular Mechanism of Neurodegeneration, Milano 2007

7 References

1. Ghindilis, A.L., Atanasov, P., Wilkins, M. and Wilkins, E.: Biosens Bioelectron. 13, 113-131 (1998)
2. Chu, X., Lin, Z.H., Shen, G.L. and Yu, R.Q.: Analyst. 120, 2829-2832 (1995)
3. Abdel-Hamid, I., Ivnitski, D., Atanasov, P. and Wilkins, E.: Biosens Bioelectron. 14, 309-316 (1999)
4. Jung, L.S., Nelson, K.E., Campbell, C.T., Stayton, P.S., Yee, S.S., Perez-Luna, V. and Lopez, G.P.: Sens. Actuators B. 54, 137-144 (1999)
5. Myszka, D.G.: J. Mol. Recognit. 12, 390-408 (1999)
6. Goodrich, T.T., Lee, H.J. and Corn, R.M.: Anal. Chem. 76, 6173-6178 (2004)
7. Karlsson, O.P. and Lofas, S.: Anal. Biochem. 300, 132-138 (2002)
8. McGill, A., Greensill, J., Marsh, R., Craft, A.W. and Toms, G.L.: J. Med. Vir. 74, 492-498 (2004)
9. Vaisocherová, H., Zítová, A., Lachmanová, M., Štěpának, J., Rosenberg, I., Králíková, Š., Liboska, R., Rejman, D. and Homola, J.: Biopolymers (2006)
10. Binz, H.K., Amstutz, P., Kohl, A., Stumpp, M.T., Briand, C., Forrer, P., Grutter, M.G. and Pluckthun, A.: Nat. Biotechnol. 22, 575-582 (2004)
11. Morton, T.A. and Myszka, D.G.: Ener. Biol. Macromol. 295, 268-+ (1998)
12. Shuman, C.F., Hamalainen, M.D. and Danielson, U.H.: J. Mol. Recog. 17, 106-119 (2004)
13. Van Der Geld, Y.M., Limburg, P.C. and Kallenberg, C.G.M.: Clin. Exp. Immunol. 118, 487-496 (1999)
14. Huang, L., Reekmans, G., Saerens, D., Friedt, J.M., Frederix, F., Francis, L., Muyldermans, S., Campitelli, A. and Hoof, C.V.: Biosens. Bioelectron. 21, 483-490 (2005)
15. Masson, J.F., Obando, L., Beaudoin, S. and Booksh, K.: Talanta. 62, 865-870 (2004)
16. Trevino, J., Calle, A., Rodriguez-Frade, J.M., Mellado, M. and Lechuga, L.M.: Anal. Chim. Acta. 647, 202-209 (2009)
17. Wittekindt, C., Fleckenstein, B., Wiesmuller, K., Eing, B.R. and Kuhn, J.E.: J. Virol. Methods. 87, 133-144 (2000)

18. Farre, M., Martinez, E., Ramon, J., Navarro, A., Radjenovic, J., Mauriz, E., Lechuga, L., Marco, M.P. and Barcelo, D.: Anal. Bioanal. Chem. 388, 207-214 (2007)
19. Lazcka, O., Del Campo, F.J. and Munoz, F.X.: Biosens Bioelectron. 22, 1205-1217 (2007)
20. Soh, N., Tokuda, T., Watanabe, T., Mishima, K., Imato, T., Masadome, T., Asano, Y., Okutani, S., Niwa, O. and Brown, S.: Talanta. 60, 733-745 (2003)
21. Lan, Y.B., Wang, S.Z., Yin, Y.G., Hoffmann, W.C. and Zheng, X.Z.: J. Bionic Eng. 5, 239-246 (2008)
22. Lotierzo, M., Henry, O.Y.F., Piletsky, S., Tothill, I., Cullen, D., Kania, M., Hock, B. and Turner, A.P.F.: Biosen.s Bioelectron. 20, 145-152 (2004)
23. Moeller, N., Mueller-Seitz, E., Scholz, O., Hillen, W., Bergwerff, A.A. and Petz, M.: Eur. Food Res. Technol. 224, 285-292 (2007)
24. Homola, J., Yee, S.S. and Myszka, D.: Surface plasmon biosensors, in book Optical Biosensors: Present and Future, (F.S. Ligler ed.) Elsevier, Amsterdam.(2002)
25. Homola, J.: Surface Plasmon Resonance Based Sensors. Springer Series on Chemical Sensors and Biosensors,O.S. Wolfbeis, Springer-Verlag, Berlin-Heidelberg-New York (2006)
26. Lofas, S., Malmqvist, M., Ronnberg, I., Stenberg, E., Liedberg, B. and Lundstrom, I.: Sens. Actuators, B. 5, 79-84 (1991)
27. Bonroy, K., Frederix, F., Reekmans, G., Dewolf, E., De Palma, R., Borghs, G., Declerck, P. and Goddeeris, B.: J. Immunol. Methods. 312, 167-181 (2006)
28. Townsend, S., Finlay, W.J.J., Hearty, S. and O'Kennedy, R.: Biosens. Bioelectron. 22, 268-274 (2006)
29. Wegner, G.J., Lee, H.J. and Corn, R.M.: Anal. Chem. 74, 5161-5168 (2002)
30. Jayasena, S.D.: Clinical Chemistry. 45, 1628-1650 (1999)
31. Wang, Z.Z., Wilkop, T., Xu, D.K., Dong, Y., Ma, G.Y. and Cheng, Q.: Anal. Bioanal. Chem. 389, 819-825 (2007)
32. Hansen, D.E.: Biomaterials. 28, 4178-4191 (2007)
33. Nuzzo, R.G. and Allara, D.L.: J. Am. Chem. Soc. 105, 4481-4483 (1983)
34. Lahiri, J., Isaacs, L., Tien, J. and Whitesides, G.M.: Anal. Chem. 71, 777-790 (1999)
35. Wang, H., Chen, S.F., Li, L.Y. and Jiang, S.Y.: Langmuir. 21, 2633-2636 (2005)

36. Koubova, V., Brynda, E., Karasova, L., Skvor, J., Homola, J., Dostalek, J., Tobiska, P. and Rosicky, J.: Sens. Actuators, B. 74, 100-105 (2001)
37. Busse, S., Scheumann, V., Menges, B. and Mittler, S.: Biosens. Bioelectron. 17, 704-710 (2002)
38. Tombelli, S., Mascini, M. and Turner, A.P.F.: Biosens. Bioelectron. 17, 929-936 (2002)
39. Lee, J.M., Park, H.K., Jung, Y., Kim, J.K., Jung, S.O. and Chung, B.H.: Anal. Chem. 79, 2680-2687 (2007)
40. Willard, F.S. and Siderovski, D.P.: Anal. Biochem. 353, 147-149 (2006)
41. Ladd, J., Boozer, C., Yu, Q.M., Chen, S.F., Homola, J. and Jiang, S.: Langmuir. 20, 8090-8095 (2004)
42. Lofas, S., Johnsson, B., Edstrom, A., Hansson, A., Lindquist, G., Hillgren, R.M.M. and Stigh, L.: Biosen.s Bioelectron. 10, 813-822 (1995)
43. Sikavitsas, V., Nitsche, J.M. and Mountziaris, T.J.: Biotechnol. Prog. 18, 885-897 (2002)
44. Jung, L.S., Nelson, K.E., Stayton, P.S. and Campbell, C.T.: Langmuir. 16, 9421-9432 (2000)
45. Homola, J.: Chemical Reviews. 108, 462-493 (2008)
46. Bamdad, C.: Biophys. J. 75, 1989-1996 (1998)
47. Peterson, A.W., Heaton, R.J. and Georgiadis, R.M.: Nucleic Acids Res. 29, 5163-5168 (2001)
48. Nelson, K.E., Gamble, L., Jung, L.S., Boeckl, M.S., Naeemi, E., Golledge, S.L., Sasaki, T., Castner, D.G., Campbell, C.T. and Stayton, P.S.: Langmuir. 17, 2807-2816 (2001)
49. Niemeyer, C.M., Burger, W. and Hoedemakers, R.M.J.: Biocon. Chem. 9, 168-175 (1998)
50. Hendrickson, W.A., Pahler, A., Smith, J.L., Satow, Y., Merritt, E.A. and Phizackerley, R.P.: Proc. Natl. Acad. Sci. U. S. A. 86, 2190-2194 (1989)
51. OShannessy, D.J. and Winzor, D.J.: Anal. Biochem. 236, 275-283 (1996)
52. Ward, L.D. and Winzor, D.J.: Anal. Biochem. 285, 179-193 (2000)
53. Oshannessy, D.J., Brighamburke, M., Soneson, K.K., Hensley, P. and Brooks, I.: Anal. Biochem. 212, 457-468 (1993)
54. www.le.ac.uk

55. Watson, J.D. and Crick, F.H.C.: Nature. 171, 737-738 (1953)
56. Hoogsteen, K.: Acta Crystallogr. 16, 907-& (1963)
57. Praseuth, D., Guieysse, A.L. and Helene, C.: Biochim. Biophys. Acta. 1489, 181-206 (1999)
58. Stojic, L., Brun, R. and Jiricny, J.: DNA Repair. 3, 1091-1101 (2004)
59. Dong, F., Allawi, H.T., Anderson, T., Neri, B.P. and Lyamichev, V.I.: Nucleic Acids Res. 29, 3248-3257 (2001)
60. www.ucl.ac.uk
61. James, P.L., Brown, T. and Fox, K.R.: Nucleic Acids Res. 31, 5598-5606 (2003)
62. Williams, M.C., Wenner, J.R., Rouzina, L. and Bloomfield, V.A.: Biophys. J. 80, 874-881 (2001)
63. www.cbs.dtu.dk
64. Lee, H.J., Goodrich, T.T. and Corn, R.M.: Anal. Chem. 73, 5525-5531 (2001)
65. Persson, B., Stenhag, K., Nilsson, P., Larsson, A., Uhlen, M. and Nygren, P.A.: Anal. Biochem. 246, 34-44 (1997)
66. Galletti, R., Masciarelli, S., Conti, C., Matusali, G., Di Renzo, L., Meschini, S., Arancia, G., Mancini, C. and Mattia, E.: Antivir. Res. 74, 102-110 (2007)
67. Uhlmann, E. and Peyman, A.: Chem. Rev. 90, 543-584 (1990)
68. Bates, P.J., Reddoch, J.F., Hansakul, P., Arrow, A., Dale, R. and Miller, D.M.: Anal. Biochem. 307, 235-243 (2002)
69. Cho, Y.K., Kim, S., Kim, Y.A., Lim, H.K., Lee, K., Yoon, D.S., Lim, G., Pak, Y.E., Ha, T.H. and Kim, K.: J. Colloid Interface Sci. 278, 44-52 (2004)
70. Zhao, Y., Kan, Z.Y., Zeng, Z.X., Hao, Y.H., Chen, H. and Tan, Z.: J. Am. Chem. Soc. 126, 13255-13264 (2004)
71. Sugimoto, N., Wu, P., Hara, H. and Kawamoto, Y.: Biochemistry. 40, 9396-9405 (2001)
72. Gao, Y., Wolf, L.K. and Georgiadis, R.M.: Nucleic Acids Res. 34, 3370-3377 (2006)
73. Chen, C.L., Wang, W.J., Ge, J. and Zhao, X.S.: Nucleic Acids Res. 37, 3756-3765 (2009)
74. Mocanu, D., Kolesnychenko, A., Aarts, S., Dejong, A.T., Pierik, A., Coene, W., Vossenaar, E. and Stapert, H.: Anal. Biochem. 380, 84-90 (2008)

75. Dai, H.Y., Meyer, M., Stepaniants, S., Ziman, M. and Stoughton, R.: Nucleic Acids Res. 30, - (2002)
76. Tawa, K. and Knoll, W.: Nucleic Acids Res. 32, 2372-2377 (2004)
77. Hagan, M.F. and Chakraborty, A.K.: J. Chem. Phys. 120, 4958-4968 (2004)
78. Lang, B.E. and Schwarz, F.P.: Biophys. Chem. 131, 96-104 (2007)
79. Okahata, Y., Kawase, M., Niikura, K., Ohtake, F., Furusawa, H. and Ebara, Y.: Anal. Chem. 70, 1288-1296 (1998)
80. Peterson, A.W., Wolf, L.K. and Georgiadis, R.M.: J. Am. Chem. Soc. 124, 14601-14607 (2002)
81. Keighley, S.D., Li, P., Estrela, P. and Mighorato, P.: Biosens. Bioelectron. 23, 1291-1297 (2008)
82. Xu, F., Pellino, A.M. and Knoll, W.: Thin Solid Films. 516, 8634-8639 (2008)
83. Srinivas, P.R., Kramer, B.S. and Srivastava, S.: Lancet Oncology. 2, 698-704 (2001)
84. Srinivas, P.R., Verma, M., Zhao, Y.M. and Srivastava, S.: Clin. Chem. 48, 1160-1169 (2002)
85. Andreescu, S. and Sadik, O.A.: Pure Appl. Chem. 76, 861-878 (2004)
86. Pejcic, B., De Marco, R. and Parkinson, G.: Analyst. 131, 1079-1090 (2006)
87. Frey, H.J., Mattila, K.M., Korolainen, M.A. and Pirttila, T.: Neurochem. Res. 30, 1501-1510 (2005)
88. Ibach, B., Binder, H., Dragon, M., Poljansky, S., Haen, E., Schmitz, E., Koch, H., Putzhammer, A., Kluenemann, H., Wieland, W. and Hajak, G.: Neurobiol. Aging. 27, 1202-1211 (2006)
89. Galasko, D., Hansen, L.A., Katzman, R., Wiederholt, W., Masliah, E., Terry, R., Hill, R., Lessin, P. and Thal, L.J.: Arch. Neurol. 51, 888-895 (1994)
90. Mckhann, G., Drachman, D., Folstein, M., Katzman, R., Price, D. and Stadlan, E.M.: Neurology. 34, 939-944 (1984)
91. Hyman, B.T. and Trojanowski, J.Q.: J. Neuropathol. Exp. Neurol. 56, 1095-1097 (1997)
92. Mirra, S.S., Heyman, A., Mckeel, D., Sumi, S.M., Crain, B.J., Brownlee, L.M., Vogel, F.S., Hughes, J.P., Vanbelle, G. and Berg, L.: Neurology. 41, 479-486 (1991)
93. www.alzheimer.ca

94. Huang, X.D., Moir, R.D., Tanzi, R.E., Bush, A.I. and Rogers, J.T.: Redox-Active Met. Neurol. Dis. 1012, 153-163 (2004)
95. Liu, G.J., Huang, W.D., Moir, R.D., Vanderburg, C.R., Lai, B., Peng, Z.C., Tanzi, R.E., Rogers, J.T. and Huang, X.D.: J. Struct. Biol. 155, 45-51 (2006)
96. Wirths, O., Multhaup, G. and Bayer, T.A.: J. Neurochem. 91, 513-520 (2004)
97. Lovell, M.A., Xiong, S.L., Markesbery, W.R. and Lynn, B.C.: Neurochem. Res. 30, 113-122 (2005)
98. Parihar, M.S. and Brewer, G.J.: Am. J. Physiol. 292, C8-C23 (2007)
99. Oppermann, U.C.T., Salim, S., Tjernberg, L.O., Terenius, L. and Jornvall, H.: FEBS Lett. 451, 238-242 (1999)
100. Yan, Y.L., Liu, Y.Z., Sorci, M., Belfort, G., Lustbader, J.W., Yan, S.S. and Wang, C.Y.: Biochemistry. 46, 1724-1731 (2007)
101. Murakami, Y., Ohsawa, I., Kasahara, T. and Ohta, S.: Neurobiol. of Aging. 30, 325-329 (2009)
102. He, X.Y., Wen, G.Y., Merz, G., Lin, D.W., Yang, Y.Z., Mehta, P., Schulz, H. and Yang, S.Y.: Mol. Brain Res. 99, 46-53 (2002)
103. Yan, S.D. and Stern, D.M.: Int. J. Exp. Pathol. 86, 161-171 (2005)
104. He, X.Y., Schulz, H. and Yang, S.Y.: J. Biol. Chem. 273, 10741-10746 (1998)
105. Yan, S.D., Fu, J., Soto, C., Chen, X., Zhu, H.J., AlMohanna, F., Collison, K., Zhu, A.P., Stern, E., Saido, T., Tohyama, M., Ogawa, S., Roher, A. and Stern, D.: Nature. 389, 689-695 (1997)
106. Sambamurti, K. and Lahiri, D.K.: Biochem. Biophys. Res. Commun. 249, 546-549 (1998)
107. Shafqat, N., Marschall, H.U., Filling, C., Nordling, E., Wu, X.Q., Bjork, L., Thyberg, J., Martensson, E., Salim, S., Jornvall, H. and Oppermann, U.: Biochem. J. 376, 49-60 (2003)
108. He, X.Y., Merz, G., Yang, Y.Z., Mehta, P., Schulz, H. and Yang, S.Y.: Eur. J. Biochem. 268, 4899-4907 (2001)
109. Marques, A.T., Antunes, A., Fernandes, P.A. and Ramos, M.J.: Bmc Genomics. 7, - (2006)
110. Lukacik, P., Kavanagh, K.L. and Oppermann, U.: Mol. Cell. Endocrinol. 248, 61-71 (2006)

111. Yang, S.Y., He, X.Y. and Schulz, H.: Trends Endocrinol. Metab. 16, 167-175 (2005)

112. Ofman, R., Ruiter, J.P.N., Feenstra, M., Duran, M., Poll-The, B.T., Zschocke, J., Ensenauer, R., Lehnert, W., Sass, J.O., Sperl, W. and Wanders, R.J.A.: Am. J. Hum. Genet. 72, 1300-1307 (2003)

113. Kretschm.E and Raether, H.: Zeit. Naturforsch. 23, 2135-& (1968)

114. Nenninger, G.G., Piliarik, M. and Homola, J.: Meas Sci Technol. 13, 2038-2046 (2002)

115. Su, X.D., Wu, Y.J., Robelek, R. and Knoll, W.: Langmuir. 21, 348-353 (2005)

116. Situma, C., Hashimoto, M. and Soper, S.A.: Biomol. Eng. 23, 213-231 (2006)

117. Jonsson, M., Anderson, H., Lindberg, U. and Aastrup, T.: Sens. Actuators, B. 123, 21-26 (2007)

118. Herne, T.M. and Tarlov, M.J.: J. Am. Chem. Soc. 119, 8916-8920 (1997)

119. Hegnerova, K., Bockova, M., Vaisocherova, H., Kristofikova, Z., Ricny, J., Ripova, D. and Homola, J.: Sens. Actuators, B. 139, 69-73 (2009)

120. Krištofiková, Z., Bocková, M., Hegnerová, K., Bartoš, A., Klaschka, J., Říčný, J., Řípová, D. and J., H.: Mol. Biosyst. in print, available online, DOI: 10.1039/b904799a

I consent to the lending of this work for study purposes and kindly ask for evidence of borrowers.

Svoluji k zapůjčení této práce pro studijní účely a prosím, aby byla řadně vedena evidence vypůjčovatelů.

Name and Surname **Address** Jméno a příjmení Adresa	**Number of ID card** Číslo OP	**Date** Datum	**Note** Poznámka